Kobe University Repository : Kernel

PDF issue: 2026-11-10

Novel strategy for anchorage position control of GPI-attached proteins in the yeast cell wall using different GPI-anchoring domains

Inokuma, Kentaro ; Kurono, Hiroki ; den Haan, Riaan ; van Zyl, Willem Heber ; Hasunuma, Tomohisa ; Kondo, Akihiko

(Citation)
Metabolic Engineering,57:110-117

(Issue Date)
2020-01

(Resource Type)
journal article

(Version)
Accepted Manuscript

(Rights)
© 2020 Elsevier.
This manuscript version is made available under the CC-BY-NC-ND 4.0 license
http://creativecommons.org/licenses/by-nc-nd/4.0/

(URL)
https://hdl.handle.net/20.500.14094/90006595

KOBE UNIVERSITY

Manuscript Details

Manuscript number	MBE_2019_253_R1
Title	Novel strategy for anchorage position control of GPI-attached proteins in the yeast cell wall using different GPI-anchoring domains
Article type	Research paper

Abstract

The yeast cell surface provides space to display functional proteins. Heterologous proteins can be covalently anchored to the yeast cell wall by fusing them with the anchoring domain of glycosylphosphatidylinositol (GPI)-anchored cell wall proteins (GPI-CWPs). In the yeast cell-surface display system, the anchorage position of the target protein in the cell wall is an important factor that maximizes the capabilities of engineered yeast cells because the yeast cell wall consists of a 100- to 200-nm-thick microfibrillar array of glucan chains. However, knowledge is limited regarding the anchorage position of GPI-attached proteins in the yeast cell wall. Here, we report a comparative study on the effect of GPI-anchoring domain–heterologous protein fusions on yeast cell wall localization. GPI-anchoring domains derived from well-characterized GPI-CWPs, namely Sed1p and Sag1p, were used for the cell-surface display of heterologous proteins in the yeast Saccharomyces cerevisiae. Immunoelectron-microscopic analysis of enhanced green fluorescent protein (eGFP)-displaying cells revealed that the anchorage position of the GPI-attached protein in the cell wall could be controlled by changing the fused anchoring domain. eGFP fused with the Sed1-anchoring domain predominantly localized to the external surface of the cell wall, whereas the anchorage position of eGFP fused with the Sag1-anchoring domain was mainly inside the cell wall. We also demonstrate the application of the anchorage position control technique to improve the cellulolytic ability of cellulase-displaying yeast. The ethanol titer during the simultaneous saccharification and fermentation of hydrothermally-processed rice straw was improved by 30% after repositioning the exo- and endo-cellulases using Sed1- and Sag1-anchor domains. This novel anchorage position control strategy will enable the efficient utilization of the cell wall space in various fields of yeast cell-surface display technology.

Keywords	Saccharomyces cerevisiae; yeast surface display; glycosylphosphatidylinositol-anchored cell wall protein; anchorage position; Sed1p; Sag1p
Taxonomy	Cellulase, Saccharomyces cerevisiae, Applied Microbiology, Fungal Cell Wall, Cell Surface Protein

Corresponding Author	Akihiko Kondo
Corresponding Author's Institution	Kobe University
Order of Authors	Kentaro Inokuma, Hiroki Kurono, Riaan Den Haan, Willem Heber van Zyl, Tomohisa Hasunuma, Akihiko Kondo

Suggested reviewers	Virendra Bisaria, Zongjun Du, Huimin Zhao, Aloia Romaní, Xinqing Zhao

Submission Files Included in this PDF

File Name [File Type]

cover letter R 191015.docx [Cover Letter]

Response to reviewers191015.docx [Response to Reviewers]

Manuscript_R191015.docx [Revised Manuscript with Changes Marked]

Highlights.docx [Highlights]

Manuscript_R191015_crear.docx [Manuscript File]

Graphical_abstract.tif [Figure]

Fig1.tif [Figure]

Fig2.tif [Figure]

Fig3.tif [Figure]

Fig4.tif [Figure]

Supplementary_materials_R.docx [e-Component]

To view all the submission files, including those not included in the PDF, click on the manuscript title on your EVISE Homepage, then click 'Download zip file'.

KOBE UNIVERSITY

Akihiko Kondo
Graduate School of Science, Technology and Innovation,
1-1 Rokkodai, Nada, Kobe 657-8501, Japan
Tel. +81-78-803-6196 Fax. +81-78-803-6196
E-mail: akondo@kobe-u.ac.jp

October 15, 2019

Dear Professor Jay Keasling,

MBE_2019_253: Kentaro Inokuma, Hiroki Kurono, Riaan den Haan, Willem Heber van Zyl, Tomohisa Hasunuma, and Akihiko Kondo; Novel strategy for anchorage position control of GPI-attached proteins in the yeast cell wall using different GPI-anchoring domains.

Thank you very much for your mail dated on September 25, 2019 together with the comments of reviewers. We have studied their comments carefully, conducted an additional experiment, and have made necessary corrections.

The following changes are our response to the comments of reviewers. The text has been revised to accommodate the comments. These changes were highlighted using red fonts in the revised manuscript.

Sincerely,

Akihiko Kondo
Graduate School of Science, Technology and Innovation, Kobe University
1-1 Rokkodai-cho, Nada-ku, Kobe 657-8501, Japan
Telephone: +81-78-803-6196, Fax: +81-78-803-6196
E-mail: akondo@kobe-u.ac.jp

In response to the comments of reviewer #1

Comments

(1) Although the authors claimed significant increase in ethanol titer, I have different opinion from the authors. The increase should be 30%, not 1.3-fold. The ethanol titer using the engineering strain IS 1.3-fold of that of the control, not increased 1.3-fold.

Author's response: Thank you for pointing that out. "1.3-fold" was corrected to "30%" (line 44 in the revised manuscript).

(2) My major concern is that the results in this study only focused on two enzymes and two anchoring domains, it will be nice if the authors provide more solid data on the mechanisms or on more applications using their anchoring domain control technology. More in-depth discussion should be added on why such results were obtained, can the authors expand their study to other cell wall proteins as the source of anchoring domains? How can other researchers benefit from this study when they used other enzymes?

Author's response: We appreciate your valuable suggestion and accordingly the following sentences were added to the Discussion section (lines 362-375 and 429-435 in the revised manuscript).

"The results presented in this study suggest that yeast cells recognize GPI-anchoring domains attached to target proteins and control their anchorage positions in the cell wall. Although the anchorage mechanism of yeast GPI-CWPs liberated from the plasma membrane to the cell wall remains unclear, recent studies have suggested that plasma membrane-anchored GPI proteins Dfg5p and Dcw1p are potential candidates for cross-linking the GPI-anchor remnant and cell wall β-(1 to 6) glucan (Gonzalez et al., 2010; Orlean, 2012). These proteins are putative glycosidase/transglycosidases homologous to bacterial family 75 (Cantarel et al., 2009) and depletion of these enzymes by repressing their expression in the double-null background led to secretion of a GPI-CWP into the medium (Kitagaki et al., 2002). These enzymes might recognize differences in GPI anchoring domains and be involved in controlling the anchorage position of GPI-attached proteins. Further analysis using GPI-anchoring domains derived from other GPI-CWPs are urgently required to identify the determinants of the

anchorage position of GPI-attached proteins. On the other hand, in order to expand this research to a wide range of GPI-CWPs, it will be necessary to develop a novel method for high-throughput anchorage position analysis."

"The anchorage position control technique demonstrated in this study will also benefit applications of yeast cell-surface display other than the construction of cellulase-displaying yeast. The hydrolysis efficiency of other plant-derived polysaccharides such as hemicellulase and starch may be improved by this technique because the complete hydrolysis of these polysaccharides also requires the cooperation of endo- and exo-type enzymes. In addition, the Sed1-anchoring domain that can expose the target protein to the external surface of the cell wall will also be a potential anchor candidate for protein screening requiring contact with large ligands."

In accordance with these additions, new references were added to the reference list (lines 473-475, 493-495, and 525-528 in the revised manuscript).

(3) How many cells have the authors observed for cell wall localization studies?

Author's response: In the immunoelectron-microscopic analysis, we observed 12 cells for each of strains BY-eGFP-SSS and BY-eGFP-SSA, and confirmed that the number and localization tendency of eGFP in the cell wall were clearly different between these strains. To make it clearer, the following sentence was added to section 3.2 (lines 249-250 in the revised manuscript).

"We observed 12 cells for each of strains BY-eGFP-SSS and BY-eGFP-SSA."

(4) How did the author evaluate the ethanol fermentation results with the previous studies? Can the authors integrate their results with their previous ones displaying more cellulosic enzymes?

Author's response: As the reviewer mentioned, we previously reported simultaneous saccharification and fermentation from pretreated rice straw using a recombinant yeast strain, in which BGL1, EGII, CBH1, and CBH2 were co-displayed using the Sed1-anchoring domain (Liu et al., 2016). Although it is not possible to fully integrate our

result (Fig. 4) with the result in the previous study due to differences in fermentation scale and agitation procedure, the BGL, EG, and CBHs co-displaying strain achieved approximately 9.5 g/L of ethanol production after 96 h fermentation with 0.2 FPU/g biomass of commercial cellulase cocktail (Liu et al., 2016). This ethanol titer is higher than that of BY-ESBA strain with 0.4 FPU/g biomass of commercial cellulase cocktail shown in Fig. 4 (7.3 g/L at 96 h). These results suggest the importance of co-display of BGL, EG, and CBHs for efficient hydrolysis of lignocellulosic biomass.

Some descriptions to contextualize this result with those we reported previously were added to the Discussion section (lines 416-428 in the revised manuscript).

(5) Line 239-240, more fluorescence was observed in the intracellular vacuoles of strain BY-eGFP-SSA than in those of strain BY-eGFP-SSS, please confirm, is the word "vacuoles" correct?

Author's response: Thank you for pointing that out. We checked several published papers and found that the word "vacuoles" was commonly used as the plural form of vacuole. As shown in Fig. 2A, we observed multiple cells containing a vacuole. Therefore, we would like to keep the word "vacuoles" in this sentence.

(6) Fig. S1, the C-terminal GPI attachment site (the ω site) marked in bold…here the sentence should be …was marked in bold.

Author's response: "marked in bold" was corrected to "was marked in bold" according to the suggestion (line 649 in the revised manuscript and page 6 line 2 in the revised Supplementary materials).

In response to the comments of reviewer #2

Comments

(1) As EG II is endoglucanase, it will have limited action on cellulose. Both CBH and EG are required for efficient hydrolysis of insoluble cellulose. Since only EG II has been used in this work, it will produce cellodextrins which may be poorly hydrolysed by beta-G. This may be the reason for low yield of ethanol by BY-ESBA strain in SSF. The authors may like to mention this point in

Discussion.

Author's response: We appreciate this valuable suggestion. The following sentences were subsequently added to the Discussion section (lines 409-428 in the revised manuscript).

"In this study, we used EG and BGL co-displaying strains for the simultaneous saccharification and fermentation of pretreated rice straw. It has been demonstrated that synergistic cooperation of EG and cellobiohydrolases (CBHs) is essential for efficient degradation of insoluble cellulose (Jalak et al. 2012). CBHs are chain end-specific processive exo-glucanases. EG randomly hydrolyzes amorphous regions of insoluble cellulose and generates reducing and non-reducing ends that can be attacked by CBHs, while CBHs recognize the cellulose chain ends and continuously hydrolyze crystalline regions between the amorphous parts into cellobiose units (Jalak et al. 2012). Previously, we reported a simultaneous saccharification and fermentation from pretreated rice straw using a recombinant yeast strain, in which BGL1, EGII, and CBHs (CBH1 and CBH2) were displayed using the Sed1-anchoring domain (Liu et al., 2016). Although direct comparison with the result shown in Fig. 4 is not possible due to differences in fermentation scale and agitation procedure, the BGL, EG, and CBHs co-displaying strain achieved approximately 9.5 g/L of ethanol production after 96 h fermentation with 0.2 FPU/g biomass of commercial cellulase cocktail (Liu et al., 2016). This ethanol titer is higher than that of BY-ESBS strain with 0.4 FPU/g biomass of commercial cellulase cocktail (7.3 g/L at 96 h, Fig. 4). These results also suggest the importance of co-display of BGL, EG, and CBHs for efficient hydrolysis of insoluble cellulosic materials. Additional display of CBHs on the cell surface of BY-ESBA strain will be required for further improvement of its ethanol yield from pretreated biomass. Furthermore , it will be necessary to verify the optimal anchorage position for CBHs in the cell wall to maximize synergies between cellulases."

In accordance with this change, a new reference was added to the reference list (lines 523-524 in the revised manuscript).

(2) Line 217: Did the yeast grow at 38C or 30C?

Author's response: First of all, we apologize for the incorrect description of

fermentation temperature. We mistakenly stated that the fermentation temperature was 38 °C, but it was carried out at 37 °C. We have already corrected this error (lines 217 and 296 in the revised manuscript).

In this study, cultivation to obtain yeast cells was performed at 30 °C, while simultaneous saccharification and fermentation using the obtained cells was performed at 37 °C to promote the activity of cellulases displayed on the cell surface (optimal temperature of *Aspergillus aculeatus* BGL1 and *Trichoderma reesei* EGII is 65 °C). To make it clearer, the following sentence was added to the section 3.5" (lines 296-298 in the revised manuscript).

"The fermentation was performed at 37 °C to promote the activity of cellulases displayed on the cell surface because the optimal temperature of *A. aculeatus* BGL1 and *T. reesei* EGII is 65 °C (Decker et al., 2000; Trudeau et al., 2014)."

In accordance with this change, new references were added to the reference list (lines 478-480 and 586-588 in the revised manuscript).

(3) Fig 4: Although BY-ESBA strain has been shown to be 1.3 fold better than BY-ESBS strain for ethanol production in SSF process, it would also be useful to compare the effectiveness of both BY-ESBA and BY-ESBS strains with that of control yeast strain not having any surface-displayed enzyme (but containing 0.4 FPU/g biomass). This may be suitably incorporated in M&M, results and discussion sections.

Author's response: We appreciate your valuable suggestion. According to the suggestion, we performed the SSF process from the pretreated rice straw with a control yeast strain BY4741, which is the parental strain of BY-ESBA and BY-ESBS strains, and 0.4 FPU/g biomass of commercial cellulase cocktail. As expected, the control strain showed lower ethanol production from the pretreated biomass than those of both BY-ESBA and BY-ESBS strains.

The fermentation result with BY4741 was included in Fig. 4 in the revised manuscript and some descriptions were added to section 3.5 (lines 294 and 298-301) and Figure legends (line 634), respectively.

Novel strategy for anchorage position control of GPI-attached proteins in the yeast cell wall using different GPI-anchoring domains

Kentaro Inokuma,[a] Hiroki Kurono,[a] Riaan den Haan,[b] Willem Heber van Zyl,[c] Tomohisa Hasunuma,[a,d,*] Akihiko Kondo[a,d,e,*]

[a] Graduate School of Science, Technology and Innovation, Kobe University, 1-1 Rokkodai-cho, Nada-ku, Kobe 657-8501, Japan

[b] Department of Biotechnology, University of the Western Cape, Bellville, 7530, South Africa

[c] Department of Microbiology, Stellenbosch University, Private Bag X1, Matieland, 7602, South Africa

[d] Engineering Biology Research Center, Kobe University, 1-1 Rokkodai-cho, Nada-ku, Kobe 657-8501, Japan

[e] Biomass Engineering Program, RIKEN, 1-7-22 Suehiro-cho, Tsurumi-ku, Yokohama, Kanagawa 230-0045, Japan

* Corresponding authors:

Tomohisa Hasunuma

Telephone: +81-78-803-6356, Fax: +81-78-803-6362

E-mail: hasunuma@port.kobe-u.ac.jp

Akihiko Kondo

Telephone: +81-78-803-6196, Fax: +81-78-803-6196

E-mail: akondo@kobe-u.ac.jp

Abstract

The yeast cell surface provides space to display functional proteins. Heterologous proteins can be covalently anchored to the yeast cell wall by fusing them with the anchoring domain of glycosylphosphatidylinositol (GPI)-anchored cell wall proteins (GPI-CWPs). In the yeast cell-surface display system, the anchorage position of the target protein in the cell wall is an important factor that maximizes the capabilities of engineered yeast cells because the yeast cell wall consists of a 100- to 200-nm-thick microfibrillar array of glucan chains. However, knowledge is limited regarding the anchorage position of GPI-attached proteins in the yeast cell wall. Here, we report a comparative study on the effect of GPI-anchoring domain–heterologous protein fusions on yeast cell wall localization. GPI-anchoring domains derived from well-characterized GPI-CWPs, namely Sed1p and Sag1p, were used for the cell-surface display of heterologous proteins in the yeast *Saccharomyces cerevisiae*. Immunoelectron-microscopic analysis of enhanced green fluorescent protein (eGFP)-displaying cells revealed that the anchorage position of the GPI-attached protein in the cell wall could be controlled by changing the fused anchoring domain. eGFP fused with the Sed1-anchoring domain predominantly localized to the external surface of the cell wall, whereas the anchorage position of eGFP fused with the Sag1-anchoring domain was mainly inside the cell wall. We also demonstrate the application of the anchorage position control technique to improve the cellulolytic ability of cellulase-displaying yeast. The ethanol titer during the simultaneous saccharification and fermentation of hydrothermally-processed rice straw was improved by 30% after repositioning the exo- and endo-cellulases using Sed1- and Sag1-anchor domains. This novel anchorage position control strategy will enable the efficient utilization of the cell wall space in various fields of yeast cell-surface display technology.

Keywords: *Saccharomyces cerevisiae*, yeast surface display, glycosylphosphatidylinositol-anchored cell wall protein, anchorage position, Sed1p, Sag1p

Abbreviations: BGL, β-glucosidase; BSA, bovine serum albumin; EG, endoglucanase; eGFP, enhanced green fluorescent protein; ER, endoplasmic reticulum; FPU, filter paper unit; GPCR, G protein-coupled receptor; GPI, glycosylphosphatidylinositol; GPI-CWP, GPI-anchored cell wall protein; GRAS, generally regarded as safe; nano-UPLC-MS^E, nanoscale ultra-pressure liquid chromatography electrospray ionization quadrupole time-of-flight tandem mass spectrometry; pAb, polyclonal antibody; *p*NPG, *p*-nitrophenyl-β-D-glucopyranoside; YP, yeast extract peptone

1. Introduction

The expression of functional proteins on the cell surface is a promising approach to construct cell-surface-engineered microorganisms with special functions. Cell-surface display technology can be used to address a wide range of applications such as the engineering and screening of enzymes, antibodies, or peptides (Angelini et al., 2015; Grzeschik et al., 2017; Li et al., 2007), the bioadsorption of specific molecules (Shibasaki and Ueda, 2014), and the production whole cell catalysts for bioconversion (Inokuma et al., 2018; Liu et al., 2016), biodegradation (Richins et al., 1997; Shibasaki et al., 2009), and biosensing (Tang et al., 2014; Wang et al., 2013).

Among host microorganisms employed for cell-surface display, baker's yeast (*Saccharomyces cerevisiae*) is the most frequently used to develop such systems because of the vast knowledge of its genetics, physiology, and fermentation characteristics, as well as its generally regarded as safe (GRAS) status. In yeast cell-surface display, the glycosylphosphatidylinositol (GPI)-anchoring system is the typical and most widely-used technique to immobilize heterologous proteins. In this method, a yeast cell is transformed by introducing fusion genes coding proteins of interest and the anchoring domain of the GPI-anchored cell wall protein (GPI-CWP). In the recombinant yeast cells, the fused proteins are synthesized on endoplasmic reticulum (ER)-bound ribosomes, cleaved at the C-terminal GPI attachment site (the ω site), and modified by the addition of a pre-assembled GPI anchor in the ER. Subsequently, the GPI-attached proteins leave the ER in COPII-coated vesicles and travel via the Golgi to the plasma membrane (Doering and Schekman, 1996). Finally, these proteins are liberated from the plasma membrane and become immobilized in the cell wall through covalent linkage to a β-(1 to 6) glucan via a remnant of the anchor structure (Klis et al., 1997; Lu et al., 1994).

It has been reported that the anchoring domains from different GPI-CWPs exhibit different efficiencies for the cell-surface display of target enzymes (Andreu and Del Olmo, 2018; Hamada et al., 1999). Therefore, selection of the appropriate anchoring domain for fusion with target proteins

is important for efficient cell-surface display. In previous studies, indeed, the activities of some cellulolytic enzymes fused with the Sed1-anchoring domain were found to be higher than those fused with the α-agglutinin (Sag1)-anchoring domain (Inokuma et al., 2014). However, the degree to which activity was improved by changing the anchoring domain varied greatly depending on the enzymes displayed. For the cell-surface display of *Aspergillus aculeatus* β-glucosidase 1 (BGL1), the activity of the enzyme fused with the Sed1-anchoring domain was approximately 2-fold higher than that upon fusion with the Sag1-anchoring domain. In contrast, the hydrolytic activity of *Trichoderma reesei* endoglucanase II (EGII) for water-insoluble cellulose was improved 60-fold when using the Sed1-anchoring domain compared to that with the Sag1-anchoring domain (Inokuma et al., 2014). Based on these results, we hypothesized that selection of the anchoring domain would affect not only the display efficiency of the target protein but also its localization in the cell wall.

The yeast cell wall is composed of a microfibrillar array of β-(1 to 3) glucan and β-(1 to 6) glucan chains with a thickness of 100 to 200 nm (Dupres et al., 2010). Therefore, cell wall proteins exposed to the external surface represent only a portion of the whole and the remainder are buried in the glucan layer (Van der Vaart et al., 1997). Small substrates such as cellobiose and *p*-nitrophenyl-β-D-glucopyranoside (*p*NPG) are accessible to all integrated enzymes because these substrates penetrate the cell wall. In contrast, large substrates such as water-insoluble cellulose can only access enzymes exposed on the external surface. However, to our knowledge, no comparative analysis has been reported concerning the effect of the anchoring domain on target protein localization in the yeast cell wall.

In the present study, we performed a comparative analysis of the effect of different anchoring domains on the cell wall localization of fused heterologous proteins in *S. cerevisiae*. First, the intracellular localization of enhanced green fluorescent protein (eGFP) fused with Sed1 or Sag1-anchoring domains was analyzed using a confocal fluorescence microscope. Subsequently,

immunoelectron-microscopic analysis of ultra-thin sections of the eGFP-displaying yeast cells was carried out to investigate the effect of the anchoring domains on the anchorage position of GPI-attached proteins in the cell wall. Finally, by applying the information obtained from this novel system, we successfully demonstrate improved ethanol production from pretreated lignocellulosic biomass by cellulase-displaying yeast after controlling the anchorage position of exo- and endo-cellulases using different anchoring domains.

2. Materials and Methods

2.1. Strains and media

Escherichia coli strain DH5α (Toyobo, Osaka, Japan) was used as the host for recombinant DNA manipulation. *E. coli* medium was prepared as described (Inokuma et al., 2016). The genetic properties of all yeast strains used in this study are shown in Table 1. The gene cassettes for the cell-surface display of heterologous proteins were expressed in the haploid yeast strain *S. cerevisiae* BY4741 (Life Technologies, Carlsbad, CA, USA).

The *S. cerevisiae* transformants were screened and cultivated as previously described (Inokuma et al., 2016). After 48 h of cultivation, yeast cells were harvested by centrifugation at 1000 × *g* for 5 min, washed twice with distilled water, and again centrifuged at 1000 × *g* for 5 min. The wet cell weight of the washed yeast cells was determined by weighing the cell pellet. The estimated dry cell weight of a yeast cell is approximately 0.15× its wet cell weight (Inokuma et al., 2014). Cell pellets were used for microscopic observation, immunoelectron-microscopy, enzyme assays, and ethanol fermentation.

2.2. Plasmid construction and yeast transformation

The plasmids and primers used in this study are listed in Supplementary Tables S1 and S2, respectively. The integrative plasmids for the expression of eGFP, *T. reesei* EGII, and *A. aculeatus*

BGL1 were transformed into *S. cerevisiae* by the lithium acetate method (Chen et al., 1992) and integrated into the *HIS3* locus or the 3′ noncoding region of YFL021W and YFL020C genes (I2 region) of the chromosomal DNA by homologous recombination. Details on the construction of plasmids and yeast transformation have been provided as Supplementary Text S1.

2.3. Fluorescence microscopy

Cell pellets of eGFP-expressing yeast strains were resuspended in 15 mM FM4-64 (Invitrogen Carlsbad, CA, USA) diluted in culture medium and incubated for 15 min at 150 rpm and 30 °C in the dark to stain vacuolar membranes. The cells were washed and resuspended in culture medium followed by a further 2-h incubation at 150 rpm and 30 °C in the dark. After washing twice with distilled water, the cells were observed using a confocal fluorescence microscope BZ-X810 (Keyence, Osaka, Japan) with a Nikon Plan Apo λ 100x/1.45 oil-immersion objective lens (Nikon, Tokyo, Japan) and appropriate filters for eGFP and FM4-64.

2.4. Sample preparation for immunoelectron-microscopy

Washed cell pellets were sandwiched between two copper disks and frozen in liquid propane at −175 °C. The frozen samples were freeze-substituted with acetone containing 0.2% glutaraldehyde and 2% distilled water at −80 °C for 2 days. The substituted samples were then transferred to −20 °C for 3 h and then warmed to 4 °C over 90 min. Next, they were dehydrated in anhydrous acetone and anhydrous ethanol at 4 °C. Infiltration was performed with LR white resin (London Resin Co. Ltd., Berkshire, UK) at 4 °C [ethanol:resin 50:50 for 2 h; 100% resin for 30 min; 100% resin for 30 min]. The samples were then transferred to a fresh 100% resin for embedding and the resins were polymerized at 50 °C overnight. The polymerized resins were cut into ultrathin sections of 90 nm thickness using an ultramicrotome (Ultracut CUT; Leica, Vienna, Austria) and the sections were placed on nickel grids.

159

160 **2.5. Immunostaining**

161 Ultrathin sections were incubated with the primary antibody [rabbit anti-GFP polyclonal
162 antibody (pAb)] in blocking solution [PBS containing 1% bovine serum albumin (BSA)] at 4 °C
163 overnight and washed three times with the blocking solution. Subsequently, they were incubated
164 with secondary antibody conjugated to 10-nm gold particles (goat anti-rabbit IgG pAb; BBI
165 Solutions, Cardiff, UK) at room temperature for 90 min and washed with PBS. The sections in the
166 nickel grids were placed in 2% glutaraldehyde in 0.1 M phosphate buffer (pH 7.4). After the grids
167 were dried, the sections were stained with 2% uranyl acetate for 15 min and Lead stain solution
168 (Sigma-Aldrich, St. Louis, MO, USA) for 3 min at room temperature.

169

170 **2.6. Immunoelectron-microscopy**

171 Ultrathin sections were observed using a transmission electron microscope (JEM-1400Plus;
172 JOEL Ltd., Tokyo Japan) at an acceleration voltage of 80 kV. Digital images (2048 × 2048 pixels)
173 were taken with a CCD camera (VELETA; Olympus Soft Imaging Solutions, Münster, Germany).

174

175 **2.7. Enzyme assays**

176 BGL and EG activities of washed yeast cell pellets were evaluated as described previously
177 (Inokuma et al., 2016). Briefly, BGL activity was assayed at pH 5.0 and 30 °C with 2 mM *p*NPG
178 as the substrate. One unit of BGL activity was defined as the amount of enzyme required to liberate
179 1 μmol of *p*-nitrophenol per min. EG activity for water-insoluble cellulose was assayed at pH 5.0
180 and 38 °C using AZCL-HE-Cellulose (Cellazyme C tablets; Megazyme, Bray, Ireland) as the
181 substrate.

182

183 **2.8. Quantification of the transcript levels of cellulase-encoding genes by real-time PCR**

184 The transcript levels of the genes encoding BGL1 and EGII were quantified by real-time PCR
185 as described previously (Liu et al., 2017). The primers used are listed in Supplementary Table S2.
186 Gene expression levels of target genes were normalized to those of the housekeeping actin gene,
187 *ACT1*.
188
189 **2.9. Relative quantitative analysis of cell wall-associated heterologous proteins**
190 The identification and relative quantification of heterologous proteins in the yeast cell wall were
191 performed based on precise mass measurements of tryptic peptides from each protein using
192 nanoscale ultra-pressure liquid chromatography electrospray ionization quadrupole time-of-flight
193 tandem mass spectrometry (nano-UPLC-MS^E). The extraction of cell wall-associated proteins,
194 sample preparation, and protein identification using nano-UPLC-MS^E were conducted as described
195 previously (Bamba et al., 2018) with a minor modification in which an ACQUITY UPLC Peptide
196 BEH C18 nanoACQUITY Column (75 μm × 100 mm; particle size, 1.7 μm; Waters Corporation,
197 Milford, MA, USA) was used as the analytical column.
198 LC-MS^E data processing and the relative quantitative analysis of cell wall-associated
199 heterologous proteins were performed using ProteinLynx Global SERVER v3.0 (Waters
200 Corporation) as described previously (Bamba et al., 2018).
201
202 **2.10. Simultaneous saccharification and fermentation of pretreated rice straw**
203 Rice straw was pretreated with the liquid hot water method and its insoluble fraction was then
204 subjected to four cycles of ball milling as described previously (Sasaki et al., 2015). The
205 composition of the pretreated rice straw was 43% (w/w) glucan, 2% (w/w) xylan, 42.3% (w/w) ash
206 and lignin, and 12.7% (w/w) other materials (Matano et al., 2012). The pretreated rice straw was
207 used as the substrate for simultaneous saccharification and fermentation in this study.

208 *S. cerevisiae* strains used for fermentation were cultivated at 30 °C for 48 h in 500 mL YPD
209 medium. The yeast cells were collected by centrifugation at 1000 × *g* for 10 min at 20 °C, and then
210 washed twice with distilled water. The cells were then resuspended in 10 mL yeast extract peptone
211 (YP) medium (10 g/L of yeast extract and 20 g/L of Bacto-peptone) containing 50 mM sodium
212 citrate buffer (pH 5.0), 100 g/L of pretreated rice straw, and 0.4 filter paper units (FPU)/g-biomass
213 of commercial cellulase (Cellic CTec2; Novozymes Inc., Bagsvaerd, Denmark) in a 50-mL
214 polypropylene tube (Corning Inc., Corning, NY, USA) at an initial cell concentration of 100 g wet
215 cells/L. Fermentation was initiated by the addition of yeast cells into the tube followed by axial
216 rotation using a heat block (Thermo Block Rotator SN-06BN; Nissin, Tokyo, Japan) at 35 rpm and
217 37 °C. The ethanol concentration in the fermentation medium was determined by HPLC
218 (Shimadzu, Kyoto, Japan), as described previously (Hasunuma et al., 2011).
219
220 **3. Results**
221 **3.1. Construction of eGFP-displaying or secreting *S. cerevisiae* strains**
222 To verify the localization of heterologous proteins fused with GPI-anchoring domains, gene
223 cassettes for the cell-surface display of eGFP were constructed using the *S. cerevisiae SED1*
224 promoter and two different GPI-anchoring regions derived from *S. cerevisiae SED1* or *SAG1* (Fig.
225 1A). We also constructed a gene cassette without the GPI-anchoring region for the secretory
226 production of eGFP. The plasmids containing these cassettes were integrated into the *HIS3* locus of
227 the chromosomal DNA of *S. cerevisiae* BY4741 by homologous recombination. The constructed
228 eGFP-displaying strains were used for microscopic observation and immunoelectron-microscopy.
229 For all gene cassettes used in this study, we used the secretion signal sequence derived from *S.*
230 *cerevisiae SED1* because it showed high performance with respect to the cell-surface display and
231 secretory production of heterologous proteins in our previous study (Inokuma et al., 2016).
232

3.2. Fluorescence and immunoelectron microscopic observations of eGFP-displaying cells

To evaluate the localization of heterologous proteins fused with GPI-anchoring domains, the fluorescence of eGFP-displaying strains (BY-eGFP-SSS and BY-eGFP-SSA) was observed using a confocal fluorescence microscope (Fig. 2A). In the strain carrying the Sed1-anchoring domain (BY-eGFP-SSS), most green fluorescence was observed on the cell surface. In contrast, in the strain carrying the Sag1-anchoring domain (BY-eGFP-SSA), less green fluorescence was observed on the cell surface compared to that in BY-eGFP-SSS. However, more fluorescence was observed in the intracellular vacuoles of strain BY-eGFP-SSA than in those of strain BY-eGFP-SSS. For comparison, we also conducted the same experiment on an eGFP-secreting strain (BY-eGFP-SSn). No significant fluorescence was observed either on the cell surface or in the intracellular vacuoles of cells of this strain.

To further evaluate the localization of heterologous proteins fused with GPI-anchoring domains in the cell wall, we performed an immunoelectron microscopy analysis of eGFP-displaying strains. Fixed BY-eGFP-SSS and BY-eGFP-SSA cell samples were cut into ultrathin sections, which were then immunostained with the primary antibody (rabbit-anti GFP) and the secondary antibody (goat anti-rabbit IgG) conjugated with 10-nm gold particles, as described in the Materials and Methods section. Immunoelectron micrographs of these strains are shown in Fig. 2B. We observed 12 cells for each of strains BY-eGFP-SSS and BY-eGFP-SSA. In both strains, most gold particles, indicating the eGFP fusion proteins, were detected on the cell surface. The number of detected gold particles associated with the cell wall was higher in BY-eGFP-SSS cells than in BY-eGFP-SSA cells. This result was in good agreement with the fluorescence observations shown in Fig. 2A. Furthermore, these strains showed different localization tendencies with respect to the eGFP fusion proteins. In strain BY-eGFP-SSS (expressing eGFP-Sed1), most gold particles were detected on the external side of the cell wall, whereas in strain BY-eGFP-SSA (expressing eGFP-Sag1), a large proportion of gold particles was detected on the internal side of the cell wall.

258

259 **3.3. Construction of *S. cerevisiae* strains co-displaying exo- and endo-cellulases**

260 To demonstrate the effect of anchorage position control using different anchoring domains, we
261 applied this technology to the co-display of exo- and endo-cellulases. Gene cassettes for the cell-
262 surface display of *A. aculeatus* BGL1 with the *S. cerevisiae SED1* promoter and GPI-anchoring
263 regions derived from *S. cerevisiae SED1* or *SAG1* were constructed (Fig. 1B). The plasmids
264 containing these cassettes were integrated into the 3′ noncoding region of *YFL021W* and *YFL020C*
265 genes in the chromosomal DNA of the BY-EG-SSS strain (Inokuma et al., 2016), which is a
266 recombinant *S. cerevisiae* strain displaying *T. reesei* EGII fused with the Sed1-anchoring domain
267 (Fig. 1C), by homologous recombination. The constructed EG and BGL co-displaying strains,
268 designated BY-ESBS and BY-ESBA (i.e., containing combinations of EGII-Sed1 + BGL1-Sed1
269 and EGII-Sed1 + BGL1-Sag1, respectively), were used for enzyme assays and direct ethanol
270 production from pretreated rice straw.

271

272 **3.4. Enzyme activity and relative quantity of cell wall-associated EGII and BGL1**

273 The EG and BGL co-displaying strains (BY-ESBS and BY-ESBA) and their parental strain
274 (BY-EG-SSS) were cultivated at 30 °C for 48 h and cell-surface EG and BGL activities were
275 evaluated as described in the Methods section (Fig. 3A). In the BY-ESBS strain, in which both EG
276 and BGL were displayed using the Sed1-anchoring domain, cell-surface EG activity was
277 approximately 40% lower compared to that in its parental strain (BY-EG-SSS). In contrast, no
278 significant difference in cell-surface EG activity was observed between the parental strain and the
279 BY-ESBA strain displaying EG and BGL using Sed1- and Sag1-anchoring domains, respectively.
280 The cell-surface BGL activity of BY-ESBS was approximately 1.5-fold higher than that of BY-
281 ESBA. We also investigated the transcriptional expression levels of *T. reesei* EGII and *A. aculeatus*

BGL1 genes in these strains by quantitative real-time PCR analysis. In these strains, no significant difference was observed in the expression levels of these genes after 48 h of cultivation (Fig. 3B).

We also performed the relative quantification of cell wall-associated cellulases in BY-ESBS and BY-ESBA strains by nano-UPLC-MS^E. The amount of cell wall-associated BGL1 per unit dry cell-weight of BY-ESBS was 1.67 ± 0.14-fold higher than that in BY-ESBA (Fig. 3C), which was similar to the fold-change in cell-surface BGL activity between these strains. In contrast, cell wall-associated EGII was not detected by nano-UPLC-MS^E analysis in either strain.

3.5. Simultaneous saccharification and fermentation of pretreated rice straw

To further verify the effect of the anchorage position control of enzymes on cellulase-displaying yeast, we performed the simultaneous saccharification and fermentation of pretreated rice straw, which was subjected to hydrothermal and ball milling treatments, using strains BY-ESBS, BY-ESBA, and their parental strain BY4741. A small amount of a commercial cellulase cocktail (0.4 FPU/g-biomass) was added to the fermentation mixture to supply auxiliary cellulolytic enzymes. The fermentation was performed at 37 °C to promote the activity of cellulases displayed on the cell surface because the optimal temperature of *A. aculeatus* BGL1 and *T. reesei* EGII was 65 °C (Decker et al., 2000; Trudeau et al., 2014). As shown in Fig. 4, the use of the EG and BGL co-displaying strains resulted in increased ethanol production from the pretreated biomass compared to that with their parental strain. Furthermore, BY-ESBA improved the ethanol production more significantly than BY-ESBS.

4. Discussion

As mentioned in the Introduction, cell-surface display systems can be utilized for a wide range of applications in *S. cerevisiae*. However, as the yeast cell wall has a thickness of 100 to 200 nm (Dupres et al., 2010), the optimal position of functional proteins in the cell surface might vary

307 depending on each application. For example, in protein screening, the exposure of target proteins to
308 the external surface of the cell wall is necessary to put them in contact with large ligands.
309 Conversely, localization close to the plasma membrane might be advantageous for screening
310 procedures utilizing signaling pathways through transmembrane proteins such as G protein-coupled
311 receptors (GPCRs) (Hara et al., 2012). Furthermore, in plant biomass degradation requiring
312 multiple enzymes, proper segregation of each enzyme in the cell wall enables the efficient
313 utilization of its limited protein loading capacity. Therefore, a technology to control the localization
314 of functional proteins in the cell wall is essential to further develop yeast cell-surface display
315 systems.

316 Although several studies on the localization control of GPI-attached proteins in the cell surface
317 have been reported over the past few decades, most have focused on whether GPI proteins are
318 retained on the plasma membrane or translocated to the cell wall (Hamada et al., 1998; Nuoffer et
319 al., 1991; Orlean, 2012). It has been suggested that the distribution of GPI proteins between the
320 plasma membrane and cell wall depends on the amino acid residues within the upstream region of
321 the GPI-attachment site (the ω-minus region). If the ω-minus region includes two basic amino acids,
322 the protein will be mostly retained in the plasma membrane in a lipid-anchored form, but if the
323 dibasic motif is absent or replaced by hydrophobic residues, the primary localization of the protein
324 is the glucan layer in the cell wall (Frieman and Cormack, 2003; Hamada et al., 1999). Another
325 determinant of the distribution of GPI proteins between the plasma membrane and cell wall is the
326 presence of longer regions rich in serine and threonine residues. Amino acid stretches that are rich
327 in serine and threonine can override the dibasic motif in the ω-minus region and promote
328 localization to the cell wall (Frieman and Cormack, 2004). Terashima et al. (2003) reported a
329 change in the localization of the GPI protein Ecm33p, from the plasma membrane to the cell wall,
330 after replacing its authentic ω-minus region with that of cell wall-localized GPI proteins, Fit1p and
331 Egt2p. In contrast, Hara et al. (2012) efficiently localized a GPCR-specific peptide ligand to the

plasma membrane by fusing it with the minimum length (six amino acids including the ω site) of the membrane-associated GPI protein Yps1p and activated the yeast pheromone response pathway. To our knowledge, however, no comparative study on the final anchorage position of GPI-attached proteins liberated from the yeast plasma membrane has been reported.

In this study, we investigated the effect of the fusion of GPI-anchoring domains to heterologous proteins on their localization in yeast cells using two GPI-anchoring domains derived from well-characterized GPI-CWPs, namely Sed1p and Sag1p (Supplementary Fig. S1). As the Sed1- and Sag1-anchoring domains used in this study have hydrophobic amino acids in their ω-minus region and the serine and threonine contents are high (41.8 and 40.3%, respectively), the proteins fused with these domains were expected to be predominantly localized to the cell wall. Confocal microscopy observations using a reporter protein (eGFP) indicated that fusing the GPI-anchoring domain to eGFP promotes intracellular transportation efficiency of the fusion protein. This result is in good agreement with the results of cell-surface BGL activity measurements in a previous study (Inokuma et al., 2014). Similar anchoring domain-dependent changes in the intracellular accumulation of GPI-attached proteins were also reported in the methylotrophic yeast *Pichia pastoris* (Zhang et al., 2013). Furthermore, immunoelectron-microscopic analysis of ultra-thin sections of the eGFP-displaying yeast cells clearly indicated that the fusion of GPI-anchoring domains with eGFP also determined its final immobilized location, and in particular, the depth in the cell wall. To our knowledge, this is the first report comparing the final destination of a heterologous protein fused with different GPI-anchoring domains in the yeast cell wall. Immunoelectron-microscopic analyses of yeast cells displaying enzymes (glucoamylase and carboxymethylcellulase) fused with the Sag1-anchoring domain have been reported previously (Murai et al., 1997a; Murai et al., 1997b). In these reports, the fusion proteins were detected only on the external surface of the cell wall. These results are not consistent with our observation shown in Fig. 2B, which is likely due to a difference in the analytical methods adopted. In the current study,

357 immunostaining was carried out after the embedding and ultrathin sectioning of the cells (see
358 Materials and Methods section), whereas in previous reports, immunostaining was performed prior
359 to embedding and sectioning (Murai et al., 1997a; Murai et al., 1997b). Therefore, enzymes fused
360 with the Sag1-anchoring domain buried in the glucan layer might not have been detected in these
361 previous reports.

362 The results presented in this study suggest that yeast cells recognize GPI-anchoring domains
363 attached to target proteins and control their anchorage positions in the cell wall. Although the
364 anchorage mechanism of yeast GPI-CWPs liberated from the plasma membrane to the cell wall
365 remains unclear, recent studies have suggested that plasma membrane-anchored GPI proteins
366 Dfg5p and Dcw1p are potential candidates for cross-linking the GPI-anchor remnant and cell wall
367 β-(1 to 6) glucan (Gonzalez et al., 2010; Orlean, 2012). These proteins are putative
368 glycosidase/transglycosidases homologous to bacterial family 75 (Cantarel et al., 2009) and
369 depletion of these enzymes by repressing their expression in the double-null background led to
370 secretion of a GPI-CWP into the medium (Kitagaki et al., 2002). These enzymes might recognize
371 differences in GPI anchoring domains and be involved in controlling the anchorage position of
372 GPI-attached proteins. Further analysis using GPI-anchoring domains derived from other GPI-
373 CWPs are urgently required to identify the determinants of the anchorage position of GPI-attached
374 proteins. On the other hand, in order to expand this research to a wide range of GPI-CWPs, it will
375 be necessary to develop a novel method for high-throughput anchorage position analysis.

376 In this study, we also demonstrated the application of the localization control technique for the
377 construction of cellulase-displaying yeast. EGII, which requires contact with bulky insoluble
378 cellulose, was preferentially localized to the external surface of the cell wall by fusing it with the
379 Sed1-anchoring domain. Concomitantly, BGL1 was immobilized on the inside of the cell wall
380 using the Sag1-anchoring domain, which avoided competition with EGII for space on the outer
381 surface. As a result of the reallocation of cell wall space, cell-surface EG activity in BY-ESBA

382 (containing combinations of EGII-Sed1 + BGL1-Sag1) was almost twice that of BY-ESBS
383 (containing combinations of EGII-Sed1 + BGL1-Sed1) (Fig. 3A). Despite lower BGL1 activity
384 (Fig. 3A), BY-ESBA achieved a higher ethanol titer after the simultaneous saccharification and
385 fermentation of pretreated lignocellulosic biomass, as compared to that with BY-ESBS (Fig. 4);
386 this is likely due to the enhanced access of EGII to its polymeric substrate. These results indicate
387 the importance of the anchorage position control of target proteins in yeast cell-surface display
388 systems.

389 To investigate the status of cellulases immobilized in the yeast cell wall in more detail, we
390 performed relative quantitative analysis of cell wall-associated cellulases in BY-ESBS and BY-
391 ESBA strains by nano-UPLC-MS^E. The amount of cell wall-associated BGL1 per unit dry cell-
392 weight of BY-ESBS was 1.67-fold higher compared to that with BY-ESBA. This result indicates
393 that the difference in cell-surface BGL activity between these strains is due to differences in the
394 abundance of cell wall-associated BGL1. Although we attempted the relative quantification of cell
395 wall-associated EGII, this protein was not detected in the cell wall fractions of both strains. One
396 possible reason for this result could be the hyperglycosylation of EGII in *S. cerevisiae*. It was
397 previously reported that recombinant *T. reesei* EGII expressed in *S. cerevisiae* has a larger
398 molecular mass compared to the native enzyme produced by *T. reesei* (48 kDa) due to different
399 levels of glycosylation; moreover, a portion of recombinant EGII presents as hyperglycosylated
400 isoforms with a broad molecular mass up to 200 kDa (Qin et al., 2008). In contrast, it was reported
401 that the glycosylation level of recombinant *Aspergillus kawachii* BGLA (Genbank annotation No.
402 BAA19913), which has significant similarity (81.8%) to *A. aculeatus* BGL1 (Genbank annotation
403 No. BAA10968) produced by *S. cerevisiae*, is fairly homogenous and that this protein has an
404 apparent molecular mass of 120 kDa (Iwashita et al., 1999). In the nano-UPLC-MS^E analysis,
405 protein identification is conducted based on precise mass measurements of tryptic peptides from
406 each protein. The masses of tryptic peptides derived from EGII displayed in this study might have

been altered by variable glycosylation, and therefore, it might not have been possible to identify this enzyme by the nano-UPLC-MS^E analysis.

In this study, we used EG and BGL co-displaying strains for the simultaneous saccharification and fermentation of pretreated rice straw. It has been demonstrated that synergistic cooperation of EG and cellobiohydrolases (CBHs) is essential for efficient degradation of insoluble cellulose (Jalak et al. 2012). CBHs are chain end-specific processive exo-glucanases. EG randomly hydrolyzes amorphous regions of insoluble cellulose and generates reducing and non-reducing ends that can be attacked by CBHs, while CBHs recognize the cellulose chain ends and continuously hydrolyze crystalline regions between the amorphous parts into cellobiose units (Jalak et al. 2012). Previously, we reported a simultaneous saccharification and fermentation from pretreated rice straw using a recombinant yeast strain, in which BGL1, EGII, and CBHs (CBH1 and CBH2) were displayed using the Sed1-anchoring domain (Liu et al., 2016). Although direct comparison with the result shown in Fig. 4 is not possible due to differences in fermentation scale and agitation procedure, the BGL, EG, and CBHs co-displaying strain achieved approximately 9.5 g/L of ethanol production after 96 h fermentation with 0.2 FPU/g biomass of commercial cellulase cocktail (Liu et al., 2016). This ethanol titer is higher than that of BY-ESBS strain with 0.4 FPU/g biomass of commercial cellulase cocktail (7.3 g/L at 96 h, Fig. 4). These results also suggest the importance of co-display of BGL, EG, and CBHs for efficient hydrolysis of insoluble cellulosic materials. Additional display of CBHs on the cell surface of BY-ESBA strain will be required for further improvement of its ethanol yield from pretreated biomass. Furthermore, it will be necessary to verify the optimal anchorage position for CBHs in the cell wall to maximize synergies between cellulases.

The anchorage position control technique demonstrated in this study will also benefit applications of yeast cell-surface display other than the construction of cellulase-displaying yeast. The hydrolysis efficiency of other plant-derived polysaccharides such as hemicellulase and starch

may be improved by this technique because the complete hydrolysis of these polysaccharides also requires the cooperation of endo- and exo-type enzymes. In addition, the Sed1-anchoring domain that can expose the target protein to the external surface of the cell wall will also be a potential anchor candidate for protein screening requiring contact with large ligands.

5. Conclusions

In the present study, we provide the first experimental evidence that the anchorage position of GPI-attached heterologous proteins in the yeast cell wall can be controlled by the specific anchoring domain fused to them. A reporter protein (eGFP) was predominantly localized to the external surface of the cell wall when fused with the Sed1-anchoring domain, whereas the anchorage position of eGFP fused with the Sag1-anchoring domain was mainly inside of the cell wall. By applying this anchorage position control technique, the cellulolytic ability of the recombinant yeast strain co-displaying EG and BGL was successfully improved. Although further analyses using GPI-anchoring domains derived from a wide-range of GPI-CWPs are required to identify the determinants of GPI-attached protein anchorage positions, our novel strategy for anchorage position control will enable the efficient utilization of the cell wall space for various fields of yeast cell-surface display.

Declaration of interest

The authors declare that they have no competing interests.

Acknowledgements

This work was supported in part by a Special Coordination Fund for Promoting Science and Technology, Creation of Innovative Centers for Advanced Interdisciplinary Research Areas (Innovative BioProduction Kobe) from the Ministry of Education, Culture, Sports, Science and

457 Technology (MEXT), Japan Society for the Promotion of Science (JSPS) KAKENHI Grant
458 Number JP18K05554, and JSPS and National Research Foundation (NRF) of South Africa under
459 the JSPS - NRF Joint Research Program (NRF Grant Number 118894).
460

461 **References**

462 Andreu, C., Del Olmo, M.L., 2018. Yeast arming systems: pros and cons of different protein
463 anchors and other elements required for display. Appl Microbiol Biotechnol. 102, 2543-
464 2561. https://doi.org/10.1007/s00253-018-8827-6.

465 Angelini, A., Chen, T.F., de Picciotto, S., Yang, N.J., Tzeng, A., Santos, M.S., Van Deventer, J.A.,
466 Traxlmayr, M.W., Wittrup, K.D., 2015. Protein Engineering and Selection Using Yeast
467 Surface Display. Methods Mol Biol. 1319, 3-36. https://doi.org/10.1007/978-1-4939-
468 2748-7_1.

469 Bamba, T., Inokuma, K., Hasunuma, T., Kondo, A., 2018. Enhanced cell-surface display of a
470 heterologous protein using *SED1* anchoring system in *SED1*-disrupted *Saccharomyces*
471 *cerevisiae* strain. J Biosci Bioeng. 125, 306-310.
472 https://doi.org/10.1016/j.jbiosc.2017.09.013.

473 Cantarel, B.L., Coutinho, P.M., Rancurel, C., Bernard, T., Lombard, V., Henrissat, B., 2009. The
474 Carbohydrate-Active EnZymes database (CAZy): an expert resource for Glycogenomics.
475 Nucleic Acids Res. 37, D233-D238. https://doi.org/10.1093/nar/gkn663.

476 Chen, D.C., Yang, B.C., Kuo, T.T., 1992. One-step transformation of yeast in stationary phase.
477 Curr Genet. 21, 83- 84.

478 Decker, C.H., Visser, J., Schreier, P., 2000. β-glucosidases from five black *Aspergillus* species:
479 study of their physico-chemical and biocatalytic properties. J Agric Food Chem. 48,
480 4929-4936. https://doi.org/10.1021/jf000434d

481 Doering, T.L., Schekman, R., 1996. GPI anchor attachment is required for Gas1p transport from
482 the endoplasmic reticulum in COP II vesicles. EMBO J. 15, 182-191.
483 Dupres, V., Dufrêne, Y.F., Heinisch, J.J., 2010. Measuring cell wall thickness in living yeast cells
484 using single molecular rulers. ACS Nano. 4, 5498-5504.
485 https://doi.org/10.1021/nn101598v.
486 Frieman, M.B., Cormack, B.P., 2003. The omega-site sequence of glycosylphosphatidylinositol-
487 anchored proteins in *Saccharomyces cerevisiae* can determine distribution between the
488 membrane and the cell wall. Mol Microbiol. 50, 883-896.
489 Frieman, M.B., Cormack, B.P., 2004. Multiple sequence signals determine the distribution of
490 glycosylphosphatidylinositol proteins between the plasma membrane and cell wall in
491 *Saccharomyces cerevisiae*. Microbiology. 150, 3105-3114.
492 https://doi.org/10.1099/mic.0.27420-0.
493 Gonzalez, M., Goddard, N., Hicks, C., Ovalle, R., Rauceo, J.M., Jue, C.K., Lipke, P.N., 2010. A
494 screen for deficiencies in GPI-anchorage of wall glycoproteins in yeast. Yeast. 27, 583-
495 596. https://doi.org/10.1002/yea.1797.
496 Grzeschik, J., Hinz, S. C., Könning, D., Pirzer, T., Becker, S., Zielonka, S., Kolmar, H., 2017. A
497 simplified procedure for antibody engineering by yeast surface display: Coupling display
498 levels and target binding by ribosomal skipping. Biotechnol J. 12.
499 https://doi.org/10.1002/biot.201600454.
500 Hamada, K., Terashima, H., Arisawa, M., Yabuki, N., Kitada, K., 1999. Amino acid residues in the
501 omega-minus region participate in cellular localization of yeast
502 glycosylphosphatidylinositol-attached proteins. J Bacteriol. 181, 3886-3889.
503 Hara, K., Ono, T., Kuroda, K., Ueda, M., 2012. Membrane-displayed peptide ligand activates the
504 pheromone response pathway in *Saccharomyces cerevisiae*. J Biochem. 151, 551-557.
505 https://doi.org/10.1093/jb/mvs027.

506 Hasunuma, T., Sung, K., Sanda, T., Yoshimura, K., Matsuda, F., Kondo, A., 2011. Efficient
507 fermentation of xylose to ethanol at high formic acid concentrations by metabolically
508 engineered *Saccharomyces cerevisiae*. Appl Microbiol Biot. 90, 997-1004.
509 https://doi.org/10.1007/s00253-011-3085-x.
510 Inokuma, K., Bamba, T., Ishii, J., Ito, Y., Hasunuma, T., Kondo, A., 2016. Enhanced cell-surface
511 display and secretory production of cellulolytic enzymes with *Saccharomyces cerevisiae*
512 Sed1 signal peptide. Biotechnol Bioeng. 113, 2358-2366.
513 https://doi.org/10.1002/bit.26008.
514 Inokuma, K., Hasunuma, T., Kondo, A., 2014. Efficient yeast cell-surface display of exo- and
515 endo-cellulase using the *SED1* anchoring region and its original promoter. Biotechnol
516 Biofuels. 7, 8. https://doi.org/10.1186/1754-6834-7-8.
517 Inokuma, K., Hasunuma, T., Kondo, A., 2018. Whole cell biocatalysts using enzymes displayed on
518 yeast cell surface. In: Chang, H., (Ed.), Emerging Areas in Bioengineering. Wiley-VCH,
519 pp. 81-92.
520 Iwashita, K., Nagahara, T., Kimura, H., Takano, M., Shimoi, H., Ito, K., 1999. The *bglA* gene of
521 *Aspergillus kawachii* encodes both extracellular and cell wall-bound β-glucosidases.
522 Appl Environ Microbiol. 65, 5546-5553.
523 Jalak, J., Kurašin, M., Teugjas, H., Väljamäe, P., 2012. Endo-exo synergism in cellulose hydrolysis
524 revisited. J Biol Chem. 287, 28802-28815. https://doi.org/10.1074/jbc.M112.381624.
525 Kitagaki, H., Wu, H., Shimoi, H., Ito, K., 2002. Two homologous genes, *DCW1* (YKL046c) and
526 *DFG5*, are essential for cell growth and encode glycosylphosphatidylinositol (GPI)-
527 anchored membrane proteins required for cell wall biogenesis in *Saccharomyces*
528 *cerevisiae*. Mol Microbiol. 46, 1011-1022.
529 Klis, F.M., Caro, L.H.P., Vossen, J.H., Kapteyn, J.C., Ram, A.F.J., Montijn, R.C., VanBerkel,
530 M.A.A., VandenEnde, H., 1997. Identification and characterization of a major building

block in the cell wall of *Saccharomyces cerevisiae*. Biochem Soc Trans. 25, 856-860. https://doi.org/10.1042/bst0250856.

Li, B., Scarselli, M., Knudsen, C.D., Kim, S.K., Jacobson, K.A., McMillin, S.M., Wess, J., 2007. Rapid identification of functionally critical amino acids in a G protein-coupled receptor. Nat Methods. 4, 169-174. https://doi.org/10.1038/nmeth990.

Liu, Z., Ho, S.H., Hasunuma, T., Chang, J.S., Ren, N.Q., Kondo, A., 2016. Recent advances in yeast cell-surface display technologies for waste biorefineries. Bioresour Technol. 215, 324-333. https://doi.org/10.1016/j.biortech.2016.03.132.

Liu, Z., Inokuma, K., Ho, S.H., den Haan, R., van Zyl, W.H., Hasunuma, T., Kondo, A., 2017. Improvement of ethanol production from crystalline cellulose via optimizing cellulase ratios in cellulolytic *Saccharomyces cerevisiae*. Biotechnol Bioeng. 114, 1201-1207. https://doi.org/10.1002/bit.26252.

Lu, C.F., Kurjan, J., Lipke, P.N., 1994. A pathway for cell wall anchorage of *Saccharomyces cerevisiae* alpha-agglutinin. Mol Cell Biol. 14, 4825-4833. https://doi.org/10.1128/MCB.14.7.4825.

Matano, Y., Hasunuma, T., Kondo, A., 2012. Display of cellulases on the cell surface of *Saccharomyces cerevisiae* for high yield ethanol production from high-solid lignocellulosic biomass. Bioresour Technol. 108, 128-133. https://doi.org/10.1016/j.biortech.2011.12.144.

Murai, T., Ueda, M., Atomi, H., Shibasaki, Y., Kamasawa, N., Osumi, M., Kawaguchi, T., Arai, M., Tanaka, A., 1997a. Genetic immobilization of cellulase on the cell surface of *Saccharomyces cerevisiae*. Appl Microbiol Biotechnol. 48, 499-503.

Murai, T., Ueda, M., Yamamura, M., Atomi, H., Shibasaki, Y., Kamasawa, N., Osumi, M., Amachi, T., Tanaka, A., 1997b. Construction of a starch-utilizing yeast by cell surface engineering. Appl Environ Microbiol. 63, 1362-1366.

556 Nuoffer, C., Jeno, P., Conzelmann, A., Riezman, H., 1991. Determinants for glycophospholipid
557 anchoring of the *Saccharomyces cerevisiae* GAS1 protein to the plasma membrane. Mol
558 Cell Biol. 11, 27-37. https://doi.org/10.1128/mcb.11.1.27.
559 Orlean, P., 2012. Architecture and biosynthesis of the *Saccharomyces cerevisiae* cell wall. Genetics.
560 192, 775-818. https://doi.org/10.1534/genetics.112.144485.
561 Qin, Y., Wei, X., Liu, X., Wang, T., Qu, Y., 2008. Purification and characterization of recombinant
562 endoglucanase of *Trichoderma reesei* expressed in *Saccharomyces cerevisiae* with
563 higher glycosylation and stability. Protein expr and purif. 58, 162-167.
564 https://doi.org/10.1016/j.pep.2007.09.004.
565 Richins, R.D., Kaneva, I., Mulchandani, A., Chen, W., 1997. Biodegradation of organophosphorus
566 pesticides by surface-expressed organophosphorus hydrolase. Nat Biotechnol. 15, 984-
567 987. https://doi.org/10.1038/nbt1097-984.
568 Sasaki, K., Tsuge, Y., Sasaki, D., Teramura, H., Inokuma, K., Hasunuma, T., Ogino, C., Kondo, A.,
569 2015. Mechanical milling and membrane separation for increased ethanol production
570 during simultaneous saccharification and co-fermentation of rice straw by xylose-
571 fermenting *Saccharomyces cerevisiae*. Bioresour Technol. 185, 263-268.
572 https://doi.org/10.1016/j.biortech.2015.02.117.
573 Shibasaki, S., Kawabata, A., Tanino, T., Kondo, A., Ueda, M., Tanaka, M., 2009. Evaluation of the
574 biodegradability of polyurethane and its derivatives by using lipase-displaying arming
575 yeast. Biocontrol Sci. 14, 171-175.
576 Shibasaki, S., Ueda, M., 2014. Bioadsorption strategies with yeast molecular display technology.
577 Biocontrol Sci. 19, 157-164. https://doi.org/10.4265/bio.19.157.
578 Tang, X., Liang, B., Yi, T., Manco, G., Palchetti, I., Liu, A., 2014. Cell surface display of
579 organophosphorus hydrolase for sensitive spectrophotometric detection of *p*-nitrophenol

substituted organophosphates. Enzyme Microb Technol. 55, 107-112. https://doi.org/10.1016/j.enzmictec.2013.10.006.

Terashima, H., Hamada, K., Kitada, K., 2003. The localization change of Ybr078w/Ecm33, a yeast GPI-associated protein, from the plasma membrane to the cell wall, affecting the cellular function. FEMS Microbiol Lett. 218, 175-180. https://doi.org/10.1111/j.1574-6968.2003.tb11515.x.

Trudeau, D.L., Lee, T.M., Arnold, F.H., 2014. Engineered thermostable fungal cellulases exhibit efficient synergistic cellulose hydrolysis at elevated temperatures. Biotechnol Bioeng. 111, 2390-2397. https://doi.org/10.1002/bit.25308.

Van der Vaart, J.M., te Biesebeke, R., Chapman, J.W., Toschka, H.Y., Klis, F.M., Verrips, C.T., 1997. Comparison of cell wall proteins of *Saccharomyces cerevisiae* as anchors for cell surface expression of heterologous proteins. Appl Environ Microbiol. 63, 615-620.

Wang, H., Lang, Q., Li, L., Liang, B., Tang, X., Kong, L., Mascini, M., Liu, A., 2013. Yeast surface displaying glucose oxidase as whole-cell biocatalyst: construction, characterization, and its electrochemical glucose sensing application. Anal Chem. 85, 6107-6112. https://doi.org/10.1021/ac400979r.

Zhang, L., Liang, S., Zhou, X., Jin, Z., Jiang, F., Han, S., Zheng, S., Lin, Y., 2013. Screening for glycosylphosphatidylinositol-modified cell wall proteins in *Pichia pastoris* and their recombinant expression on the cell surface. Appl Environ Microbiol. 79, 5519-5526. https://doi.org/10.1128/AEM.00824-13.

605 **Table 1** Characteristics of yeast strains used in this study

Strains	Relevant genotype	Source
S. cerevisiae BY4741	*MAT**a** his3Δ1 leu2Δ0 met15Δ0 ura3Δ0*	Invitrogen
BY-eGFP-SSS	BY4741/pIeGFP-SSS	This study
BY-eGFP-SSA	BY4741/pIeGFP-SSA	This study
BY-eGFP-SSn	BY4741/pIeGFP-SS2	This study
BY-BG-SSS	BY4741/pIBG-SSS	Inokuma et al. (2016)
BY-EG-SSS	BY4741/pIEG-SSS	Inokuma et al. (2016)
BY-ESBS	BY-EG-SSS/pIL2BG-SSS	This study
BY-ESBA	BY-EG-SSS/pIL2BG-SSA	This study

606

607

608 **Figure legends**

609

610 **Fig. 1** Schematic summary of the construction of gene cassettes used in this study. **(A)** Gene
611 cassettes for cell-surface display and the secretory production of eGFP. **(B)** Gene cassettes for the
612 cell-surface display of BGL1. **(C)** Gene cassettes for cell-surface display of EGII.

613

614 **Fig. 2** Localization analyses of eGFP fused with Sed1- or Sag1-anchoring domains. **(A)**
615 Fluorescence images of strains BY-eGFP-SSS, BY-eGFP-SSA, and BY-eGFP-SSn. The cells
616 were incubated in YPD medium for 48 h, stained with FM4-64 (red) to visualize vacuolar
617 membranes, and then observed using a confocal microscope. **(B)** Immunoelectron micrographs of
618 strains BY-eGFP-SSS and BY-eGFP-SSA. The cells were immunogold-labeled with an antibody
619 against GFP. The arrowheads indicate gold particles.

620

621 **Fig. 3** Effects of anchorage position control on enzyme activities of cellulase-displaying yeasts. **(A)**
622 Comparison of cell-surface EG and BGL activities in strains BY-BG-SSS, BY-ESBS, and BY-
623 ESBA after cultivation in YPD medium for 48 h. The relative EG activity of each strain is shown
624 as a fold-change in EG activity relative to the average level observed with the parental strain BY-
625 EG-SSS. **(B)** Comparison of transcript levels of EGII- and BGL1-encoding genes in strains BY-
626 ESBS and BY-ESBA after cultivation in YPD medium for 48 h. The relative transcript level of
627 each gene is shown as a fold-change in mRNA levels relative to the average level detected in strain
628 BY-ESBS. **(C)** Relative quantification of BGL1 in the cell walls of strains BY-ESBS and BY-
629 ESBA by nanoscale ultra-pressure liquid chromatography electrospray ionization quadrupole time-
630 of-flight tandem mass spectrometry (nano-UPLC-MS^E). The amount of BGL1 was normalized to
631 the dry cell weight of each strain. Data are presented as the means ± standard deviation (n = 3).

632

633 **Fig. 4** Time course of the simultaneous saccharification and fermentation of 100 g dry weight/L of
634 pretreated rice straw by strains BY-ESBS, BY-ESBA, and their parental strain (BY4741). A small
635 amount of a commercial cellulase cocktail (0.4 FPU/g-biomass) was added to the fermentation
636 mixture. Data are presented as the means ± standard deviation (n = 3).
637
638
639
640

641 **Supplementary materials**

642 **Text S1** Plasmid construction and yeast transformation.

643

644 **Table S1** Characteristics of integrative plasmids used in this study.

645

646 **Table S2** PCR primers used in this study.

647

648 **Fig. S1** Amino acid sequence of Sed1- and Sag1-anchoring domains used in this study. The C-
649 terminal GPI attachment site (the ω site) was marked in bold. The hydrophobic amino acid residues
650 in the ω-minus region are underlined.

651

Highlights

- The GPI-anchoring domain fused with a heterologous protein determines its anchorage position in yeast cell wall.
- Proteins fused with the Sed1-anchoring domain predominantly localize to the external surface of the cell wall.
- The anchorage position of proteins fused with the Sag1-anchoring domain is mainly inside of the cell wall.
- By repositioning exo- and endo-cellulases in cellulase-displaying yeast, the ethanol titer from pretreated rice straw was improved by 30%.

Novel strategy for anchorage position control of GPI-attached proteins in the yeast cell wall using different GPI-anchoring domains

Kentaro Inokuma,[a] Hiroki Kurono,[a] Riaan den Haan,[b] Willem Heber van Zyl,[c] Tomohisa Hasunuma,[a,d,*] Akihiko Kondo[a,d,e,*]

[a] Graduate School of Science, Technology and Innovation, Kobe University, 1-1 Rokkodai-cho, Nada-ku, Kobe 657-8501, Japan

[b] Department of Biotechnology, University of the Western Cape, Bellville, 7530, South Africa

[c] Department of Microbiology, Stellenbosch University, Private Bag X1, Matieland, 7602, South Africa

[d] Engineering Biology Research Center, Kobe University, 1-1 Rokkodai-cho, Nada-ku, Kobe 657-8501, Japan

[e] Biomass Engineering Program, RIKEN, 1-7-22 Suehiro-cho, Tsurumi-ku, Yokohama, Kanagawa 230-0045, Japan

* Corresponding authors:

Tomohisa Hasunuma

Telephone: +81-78-803-6356, Fax: +81-78-803-6362

E-mail: hasunuma@port.kobe-u.ac.jp

Akihiko Kondo

Telephone: +81-78-803-6196, Fax: +81-78-803-6196

E-mail: akondo@kobe-u.ac.jp

Abstract

The yeast cell surface provides space to display functional proteins. Heterologous proteins can be covalently anchored to the yeast cell wall by fusing them with the anchoring domain of glycosylphosphatidylinositol (GPI)-anchored cell wall proteins (GPI-CWPs). In the yeast cell-surface display system, the anchorage position of the target protein in the cell wall is an important factor that maximizes the capabilities of engineered yeast cells because the yeast cell wall consists of a 100- to 200-nm-thick microfibrillar array of glucan chains. However, knowledge is limited regarding the anchorage position of GPI-attached proteins in the yeast cell wall. Here, we report a comparative study on the effect of GPI-anchoring domain–heterologous protein fusions on yeast cell wall localization. GPI-anchoring domains derived from well-characterized GPI-CWPs, namely Sed1p and Sag1p, were used for the cell-surface display of heterologous proteins in the yeast *Saccharomyces cerevisiae*. Immunoelectron-microscopic analysis of enhanced green fluorescent protein (eGFP)-displaying cells revealed that the anchorage position of the GPI-attached protein in the cell wall could be controlled by changing the fused anchoring domain. eGFP fused with the Sed1-anchoring domain predominantly localized to the external surface of the cell wall, whereas the anchorage position of eGFP fused with the Sag1-anchoring domain was mainly inside the cell wall. We also demonstrate the application of the anchorage position control technique to improve the cellulolytic ability of cellulase-displaying yeast. The ethanol titer during the simultaneous saccharification and fermentation of hydrothermally-processed rice straw was improved by 30% after repositioning the exo- and endo-cellulases using Sed1- and Sag1-anchor domains. This novel anchorage position control strategy will enable the efficient utilization of the cell wall space in various fields of yeast cell-surface display technology.

Keywords: *Saccharomyces cerevisiae*, yeast surface display, glycosylphosphatidylinositol-anchored cell wall protein, anchorage position, Sed1p, Sag1p

Abbreviations: BGL, β-glucosidase; BSA, bovine serum albumin; EG, endoglucanase; eGFP, enhanced green fluorescent protein; ER, endoplasmic reticulum; FPU, filter paper unit; GPCR, G protein-coupled receptor; GPI, glycosylphosphatidylinositol; GPI-CWP, GPI-anchored cell wall protein; GRAS, generally regarded as safe; nano-UPLC-MS^E, nanoscale ultra-pressure liquid chromatography electrospray ionization quadrupole time-of-flight tandem mass spectrometry; pAb, polyclonal antibody; *p*NPG, *p*-nitrophenyl-β-D-glucopyranoside; YP, yeast extract peptone

1. Introduction

The expression of functional proteins on the cell surface is a promising approach to construct cell-surface-engineered microorganisms with special functions. Cell-surface display technology can be used to address a wide range of applications such as the engineering and screening of enzymes, antibodies, or peptides (Angelini et al., 2015; Grzeschik et al., 2017; Li et al., 2007), the bioadsorption of specific molecules (Shibasaki and Ueda, 2014), and the production whole cell catalysts for bioconversion (Inokuma et al., 2018; Liu et al., 2016), biodegradation (Richins et al., 1997; Shibasaki et al., 2009), and biosensing (Tang et al., 2014; Wang et al., 2013).

Among host microorganisms employed for cell-surface display, baker's yeast (*Saccharomyces cerevisiae*) is the most frequently used to develop such systems because of the vast knowledge of its genetics, physiology, and fermentation characteristics, as well as its generally regarded as safe (GRAS) status. In yeast cell-surface display, the glycosylphosphatidylinositol (GPI)-anchoring system is the typical and most widely-used technique to immobilize heterologous proteins. In this method, a yeast cell is transformed by introducing fusion genes coding proteins of interest and the anchoring domain of the GPI-anchored cell wall protein (GPI-CWP). In the recombinant yeast cells, the fused proteins are synthesized on endoplasmic reticulum (ER)-bound ribosomes, cleaved at the C-terminal GPI attachment site (the ω site), and modified by the addition of a pre-assembled GPI anchor in the ER. Subsequently, the GPI-attached proteins leave the ER in COPII-coated vesicles and travel via the Golgi to the plasma membrane (Doering and Schekman, 1996). Finally, these proteins are liberated from the plasma membrane and become immobilized in the cell wall through covalent linkage to a β-(1 to 6) glucan via a remnant of the anchor structure (Klis et al., 1997; Lu et al., 1994).

It has been reported that the anchoring domains from different GPI-CWPs exhibit different efficiencies for the cell-surface display of target enzymes (Andreu and Del Olmo, 2018; Hamada et al., 1999). Therefore, selection of the appropriate anchoring domain for fusion with target proteins

is important for efficient cell-surface display. In previous studies, indeed, the activities of some cellulolytic enzymes fused with the Sed1-anchoring domain were found to be higher than those fused with the α-agglutinin (Sag1)-anchoring domain (Inokuma et al., 2014). However, the degree to which activity was improved by changing the anchoring domain varied greatly depending on the enzymes displayed. For the cell-surface display of *Aspergillus aculeatus* β-glucosidase 1 (BGL1), the activity of the enzyme fused with the Sed1-anchoring domain was approximately 2-fold higher than that upon fusion with the Sag1-anchoring domain. In contrast, the hydrolytic activity of *Trichoderma reesei* endoglucanase II (EGII) for water-insoluble cellulose was improved 60-fold when using the Sed1-anchoring domain compared to that with the Sag1-anchoring domain (Inokuma et al., 2014). Based on these results, we hypothesized that selection of the anchoring domain would affect not only the display efficiency of the target protein but also its localization in the cell wall.

The yeast cell wall is composed of a microfibrillar array of β-(1 to 3) glucan and β-(1 to 6) glucan chains with a thickness of 100 to 200 nm (Dupres et al., 2010). Therefore, cell wall proteins exposed to the external surface represent only a portion of the whole and the remainder are buried in the glucan layer (Van der Vaart et al., 1997). Small substrates such as cellobiose and *p*-nitrophenyl-β-D-glucopyranoside (*p*NPG) are accessible to all integrated enzymes because these substrates penetrate the cell wall. In contrast, large substrates such as water-insoluble cellulose can only access enzymes exposed on the external surface. However, to our knowledge, no comparative analysis has been reported concerning the effect of the anchoring domain on target protein localization in the yeast cell wall.

In the present study, we performed a comparative analysis of the effect of different anchoring domains on the cell wall localization of fused heterologous proteins in *S. cerevisiae*. First, the intracellular localization of enhanced green fluorescent protein (eGFP) fused with Sed1 or Sag1-anchoring domains was analyzed using a confocal fluorescence microscope. Subsequently,

immunoelectron-microscopic analysis of ultra-thin sections of the eGFP-displaying yeast cells was carried out to investigate the effect of the anchoring domains on the anchorage position of GPI-attached proteins in the cell wall. Finally, by applying the information obtained from this novel system, we successfully demonstrate improved ethanol production from pretreated lignocellulosic biomass by cellulase-displaying yeast after controlling the anchorage position of exo- and endo-cellulases using different anchoring domains.

2. Materials and Methods

2.1. Strains and media

Escherichia coli strain DH5α (Toyobo, Osaka, Japan) was used as the host for recombinant DNA manipulation. *E. coli* medium was prepared as described (Inokuma et al., 2016). The genetic properties of all yeast strains used in this study are shown in Table 1. The gene cassettes for the cell-surface display of heterologous proteins were expressed in the haploid yeast strain *S. cerevisiae* BY4741 (Life Technologies, Carlsbad, CA, USA).

The *S. cerevisiae* transformants were screened and cultivated as previously described (Inokuma et al., 2016). After 48 h of cultivation, yeast cells were harvested by centrifugation at 1000 × *g* for 5 min, washed twice with distilled water, and again centrifuged at 1000 × *g* for 5 min. The wet cell weight of the washed yeast cells was determined by weighing the cell pellet. The estimated dry cell weight of a yeast cell is approximately 0.15× its wet cell weight (Inokuma et al., 2014). Cell pellets were used for microscopic observation, immunoelectron-microscopy, enzyme assays, and ethanol fermentation.

2.2. Plasmid construction and yeast transformation

The plasmids and primers used in this study are listed in Supplementary Tables S1 and S2, respectively. The integrative plasmids for the expression of eGFP, *T. reesei* EGII, and *A. aculeatus*

BGL1 were transformed into *S. cerevisiae* by the lithium acetate method (Chen et al., 1992) and integrated into the *HIS3* locus or the 3′ noncoding region of YFL021W and YFL020C genes (I2 region) of the chromosomal DNA by homologous recombination. Details on the construction of plasmids and yeast transformation have been provided as Supplementary Text S1.

2.3. Fluorescence microscopy

Cell pellets of eGFP-expressing yeast strains were resuspended in 15 mM FM4-64 (Invitrogen Carlsbad, CA, USA) diluted in culture medium and incubated for 15 min at 150 rpm and 30 °C in the dark to stain vacuolar membranes. The cells were washed and resuspended in culture medium followed by a further 2-h incubation at 150 rpm and 30 °C in the dark. After washing twice with distilled water, the cells were observed using a confocal fluorescence microscope BZ-X810 (Keyence, Osaka, Japan) with a Nikon Plan Apo λ 100x/1.45 oil-immersion objective lens (Nikon, Tokyo, Japan) and appropriate filters for eGFP and FM4-64.

2.4. Sample preparation for immunoelectron-microscopy

Washed cell pellets were sandwiched between two copper disks and frozen in liquid propane at −175 °C. The frozen samples were freeze-substituted with acetone containing 0.2% glutaraldehyde and 2% distilled water at −80 °C for 2 days. The substituted samples were then transferred to −20 °C for 3 h and then warmed to 4 °C over 90 min. Next, they were dehydrated in anhydrous acetone and anhydrous ethanol at 4 °C. Infiltration was performed with LR white resin (London Resin Co. Ltd., Berkshire, UK) at 4 °C [ethanol:resin 50:50 for 2 h; 100% resin for 30 min; 100% resin for 30 min]. The samples were then transferred to a fresh 100% resin for embedding and the resins were polymerized at 50 °C overnight. The polymerized resins were cut into ultrathin sections of 90 nm thickness using an ultramicrotome (Ultracut CUT; Leica, Vienna, Austria) and the sections were placed on nickel grids.

159

160 **2.5. Immunostaining**

161 Ultrathin sections were incubated with the primary antibody [rabbit anti-GFP polyclonal
162 antibody (pAb)] in blocking solution [PBS containing 1% bovine serum albumin (BSA)] at 4 °C
163 overnight and washed three times with the blocking solution. Subsequently, they were incubated
164 with secondary antibody conjugated to 10-nm gold particles (goat anti-rabbit IgG pAb; BBI
165 Solutions, Cardiff, UK) at room temperature for 90 min and washed with PBS. The sections in the
166 nickel grids were placed in 2% glutaraldehyde in 0.1 M phosphate buffer (pH 7.4). After the grids
167 were dried, the sections were stained with 2% uranyl acetate for 15 min and Lead stain solution
168 (Sigma-Aldrich, St. Louis, MO, USA) for 3 min at room temperature.

169

170 **2.6. Immunoelectron-microscopy**

171 Ultrathin sections were observed using a transmission electron microscope (JEM-1400Plus;
172 JOEL Ltd., Tokyo Japan) at an acceleration voltage of 80 kV. Digital images (2048 × 2048 pixels)
173 were taken with a CCD camera (VELETA; Olympus Soft Imaging Solutions, Münster, Germany).

174

175 **2.7. Enzyme assays**

176 BGL and EG activities of washed yeast cell pellets were evaluated as described previously
177 (Inokuma et al., 2016). Briefly, BGL activity was assayed at pH 5.0 and 30 °C with 2 mM *p*NPG
178 as the substrate. One unit of BGL activity was defined as the amount of enzyme required to liberate
179 1 μmol of *p*-nitrophenol per min. EG activity for water-insoluble cellulose was assayed at pH 5.0
180 and 38 °C using AZCL-HE-Cellulose (Cellazyme C tablets; Megazyme, Bray, Ireland) as the
181 substrate.

182

183 **2.8. Quantification of the transcript levels of cellulase-encoding genes by real-time PCR**

184 The transcript levels of the genes encoding BGL1 and EGII were quantified by real-time PCR
185 as described previously (Liu et al., 2017). The primers used are listed in Supplementary Table S2.
186 Gene expression levels of target genes were normalized to those of the housekeeping actin gene,
187 *ACT1*.
188
189 **2.9. Relative quantitative analysis of cell wall-associated heterologous proteins**
190 The identification and relative quantification of heterologous proteins in the yeast cell wall were
191 performed based on precise mass measurements of tryptic peptides from each protein using
192 nanoscale ultra-pressure liquid chromatography electrospray ionization quadrupole time-of-flight
193 tandem mass spectrometry (nano-UPLC-MS^E). The extraction of cell wall-associated proteins,
194 sample preparation, and protein identification using nano-UPLC-MS^E were conducted as described
195 previously (Bamba et al., 2018) with a minor modification in which an ACQUITY UPLC Peptide
196 BEH C18 nanoACQUITY Column (75 μm × 100 mm; particle size, 1.7 μm; Waters Corporation,
197 Milford, MA, USA) was used as the analytical column.
198 LC-MS^E data processing and the relative quantitative analysis of cell wall-associated
199 heterologous proteins were performed using ProteinLynx Global SERVER v3.0 (Waters
200 Corporation) as described previously (Bamba et al., 2018).
201
202 **2.10. Simultaneous saccharification and fermentation of pretreated rice straw**
203 Rice straw was pretreated with the liquid hot water method and its insoluble fraction was then
204 subjected to four cycles of ball milling as described previously (Sasaki et al., 2015). The
205 composition of the pretreated rice straw was 43% (w/w) glucan, 2% (w/w) xylan, 42.3% (w/w) ash
206 and lignin, and 12.7% (w/w) other materials (Matano et al., 2012). The pretreated rice straw was
207 used as the substrate for simultaneous saccharification and fermentation in this study.

S. cerevisiae strains used for fermentation were cultivated at 30 °C for 48 h in 500 mL YPD medium. The yeast cells were collected by centrifugation at 1000 × *g* for 10 min at 20 °C, and then washed twice with distilled water. The cells were then resuspended in 10 mL yeast extract peptone (YP) medium (10 g/L of yeast extract and 20 g/L of Bacto-peptone) containing 50 mM sodium citrate buffer (pH 5.0), 100 g/L of pretreated rice straw, and 0.4 filter paper units (FPU)/g-biomass of commercial cellulase (Cellic CTec2; Novozymes Inc., Bagsvaerd, Denmark) in a 50-mL polypropylene tube (Corning Inc., Corning, NY, USA) at an initial cell concentration of 100 g wet cells/L. Fermentation was initiated by the addition of yeast cells into the tube followed by axial rotation using a heat block (Thermo Block Rotator SN-06BN; Nissin, Tokyo, Japan) at 35 rpm and 37 °C. The ethanol concentration in the fermentation medium was determined by HPLC (Shimadzu, Kyoto, Japan), as described previously (Hasunuma et al., 2011).

3. Results

3.1. Construction of eGFP-displaying or secreting *S. cerevisiae* strains

To verify the localization of heterologous proteins fused with GPI-anchoring domains, gene cassettes for the cell-surface display of eGFP were constructed using the *S. cerevisiae SED1* promoter and two different GPI-anchoring regions derived from *S. cerevisiae SED1* or *SAG1* (Fig. 1A). We also constructed a gene cassette without the GPI-anchoring region for the secretory production of eGFP. The plasmids containing these cassettes were integrated into the *HIS3* locus of the chromosomal DNA of *S. cerevisiae* BY4741 by homologous recombination. The constructed eGFP-displaying strains were used for microscopic observation and immunoelectron-microscopy. For all gene cassettes used in this study, we used the secretion signal sequence derived from *S. cerevisiae SED1* because it showed high performance with respect to the cell-surface display and secretory production of heterologous proteins in our previous study (Inokuma et al., 2016).

3.2. Fluorescence and immunoelectron microscopic observations of eGFP-displaying cells

To evaluate the localization of heterologous proteins fused with GPI-anchoring domains, the fluorescence of eGFP-displaying strains (BY-eGFP-SSS and BY-eGFP-SSA) was observed using a confocal fluorescence microscope (Fig. 2A). In the strain carrying the Sed1-anchoring domain (BY-eGFP-SSS), most green fluorescence was observed on the cell surface. In contrast, in the strain carrying the Sag1-anchoring domain (BY-eGFP-SSA), less green fluorescence was observed on the cell surface compared to that in BY-eGFP-SSS. However, more fluorescence was observed in the intracellular vacuoles of strain BY-eGFP-SSA than in those of strain BY-eGFP-SSS. For comparison, we also conducted the same experiment on an eGFP-secreting strain (BY-eGFP-SSn). No significant fluorescence was observed either on the cell surface or in the intracellular vacuoles of cells of this strain.

To further evaluate the localization of heterologous proteins fused with GPI-anchoring domains in the cell wall, we performed an immunoelectron microscopy analysis of eGFP-displaying strains. Fixed BY-eGFP-SSS and BY-eGFP-SSA cell samples were cut into ultrathin sections, which were then immunostained with the primary antibody (rabbit-anti GFP) and the secondary antibody (goat anti-rabbit IgG) conjugated with 10-nm gold particles, as described in the Materials and Methods section. Immunoelectron micrographs of these strains are shown in Fig. 2B. We observed 12 cells for each of strains BY-eGFP-SSS and BY-eGFP-SSA. In both strains, most gold particles, indicating the eGFP fusion proteins, were detected on the cell surface. The number of detected gold particles associated with the cell wall was higher in BY-eGFP-SSS cells than in BY-eGFP-SSA cells. This result was in good agreement with the fluorescence observations shown in Fig. 2A. Furthermore, these strains showed different localization tendencies with respect to the eGFP fusion proteins. In strain BY-eGFP-SSS (expressing eGFP-Sed1), most gold particles were detected on the external side of the cell wall, whereas in strain BY-eGFP-SSA (expressing eGFP-Sag1), a large proportion of gold particles was detected on the internal side of the cell wall.

258

259 **3.3. Construction of *S. cerevisiae* strains co-displaying exo- and endo-cellulases**

260 To demonstrate the effect of anchorage position control using different anchoring domains, we
261 applied this technology to the co-display of exo- and endo-cellulases. Gene cassettes for the cell-
262 surface display of *A. aculeatus* BGL1 with the *S. cerevisiae SED1* promoter and GPI-anchoring
263 regions derived from *S. cerevisiae SED1* or *SAG1* were constructed (Fig. 1B). The plasmids
264 containing these cassettes were integrated into the 3′ noncoding region of *YFL021W* and *YFL020C*
265 genes in the chromosomal DNA of the BY-EG-SSS strain (Inokuma et al., 2016), which is a
266 recombinant *S. cerevisiae* strain displaying *T. reesei* EGII fused with the Sed1-anchoring domain
267 (Fig. 1C), by homologous recombination. The constructed EG and BGL co-displaying strains,
268 designated BY-ESBS and BY-ESBA (i.e., containing combinations of EGII-Sed1 + BGL1-Sed1
269 and EGII-Sed1 + BGL1-Sag1, respectively), were used for enzyme assays and direct ethanol
270 production from pretreated rice straw.

271

272 **3.4. Enzyme activity and relative quantity of cell wall-associated EGII and BGL1**

273 The EG and BGL co-displaying strains (BY-ESBS and BY-ESBA) and their parental strain
274 (BY-EG-SSS) were cultivated at 30 °C for 48 h and cell-surface EG and BGL activities were
275 evaluated as described in the Methods section (Fig. 3A). In the BY-ESBS strain, in which both EG
276 and BGL were displayed using the Sed1-anchoring domain, cell-surface EG activity was
277 approximately 40% lower compared to that in its parental strain (BY-EG-SSS). In contrast, no
278 significant difference in cell-surface EG activity was observed between the parental strain and the
279 BY-ESBA strain displaying EG and BGL using Sed1- and Sag1-anchoring domains, respectively.
280 The cell-surface BGL activity of BY-ESBS was approximately 1.5-fold higher than that of BY-
281 ESBA. We also investigated the transcriptional expression levels of *T. reesei* EGII and *A. aculeatus*

BGL1 genes in these strains by quantitative real-time PCR analysis. In these strains, no significant difference was observed in the expression levels of these genes after 48 h of cultivation (Fig. 3B).

We also performed the relative quantification of cell wall-associated cellulases in BY-ESBS and BY-ESBA strains by nano-UPLC-MS^E. The amount of cell wall-associated BGL1 per unit dry cell-weight of BY-ESBS was 1.67 ± 0.14-fold higher than that in BY-ESBA (Fig. 3C), which was similar to the fold-change in cell-surface BGL activity between these strains. In contrast, cell wall-associated EGII was not detected by nano-UPLC-MS^E analysis in either strain.

3.5. Simultaneous saccharification and fermentation of pretreated rice straw

To further verify the effect of the anchorage position control of enzymes on cellulase-displaying yeast, we performed the simultaneous saccharification and fermentation of pretreated rice straw, which was subjected to hydrothermal and ball milling treatments, using strains BY-ESBS, BY-ESBA, and their parental strain BY4741. A small amount of a commercial cellulase cocktail (0.4 FPU/g-biomass) was added to the fermentation mixture to supply auxiliary cellulolytic enzymes. The fermentation was performed at 37 °C to promote the activity of cellulases displayed on the cell surface because the optimal temperature of *A. aculeatus* BGL1 and *T. reesei* EGII was 65 °C (Decker et al., 2000; Trudeau et al., 2014). As shown in Fig. 4, the use of the EG and BGL co-displaying strains resulted in increased ethanol production from the pretreated biomass compared to that with their parental strain. Furthermore, BY-ESBA improved the ethanol production more significantly than BY-ESBS.

4. Discussion

As mentioned in the Introduction, cell-surface display systems can be utilized for a wide range of applications in *S. cerevisiae*. However, as the yeast cell wall has a thickness of 100 to 200 nm (Dupres et al., 2010), the optimal position of functional proteins in the cell surface might vary

307 depending on each application. For example, in protein screening, the exposure of target proteins to
308 the external surface of the cell wall is necessary to put them in contact with large ligands.
309 Conversely, localization close to the plasma membrane might be advantageous for screening
310 procedures utilizing signaling pathways through transmembrane proteins such as G protein-coupled
311 receptors (GPCRs) (Hara et al., 2012). Furthermore, in plant biomass degradation requiring
312 multiple enzymes, proper segregation of each enzyme in the cell wall enables the efficient
313 utilization of its limited protein loading capacity. Therefore, a technology to control the localization
314 of functional proteins in the cell wall is essential to further develop yeast cell-surface display
315 systems.

316 Although several studies on the localization control of GPI-attached proteins in the cell surface
317 have been reported over the past few decades, most have focused on whether GPI proteins are
318 retained on the plasma membrane or translocated to the cell wall (Hamada et al., 1998; Nuoffer et
319 al., 1991; Orlean, 2012). It has been suggested that the distribution of GPI proteins between the
320 plasma membrane and cell wall depends on the amino acid residues within the upstream region of
321 the GPI-attachment site (the ω-minus region). If the ω-minus region includes two basic amino acids,
322 the protein will be mostly retained in the plasma membrane in a lipid-anchored form, but if the
323 dibasic motif is absent or replaced by hydrophobic residues, the primary localization of the protein
324 is the glucan layer in the cell wall (Frieman and Cormack, 2003; Hamada et al., 1999). Another
325 determinant of the distribution of GPI proteins between the plasma membrane and cell wall is the
326 presence of longer regions rich in serine and threonine residues. Amino acid stretches that are rich
327 in serine and threonine can override the dibasic motif in the ω-minus region and promote
328 localization to the cell wall (Frieman and Cormack, 2004). Terashima et al. (2003) reported a
329 change in the localization of the GPI protein Ecm33p, from the plasma membrane to the cell wall,
330 after replacing its authentic ω-minus region with that of cell wall-localized GPI proteins, Fit1p and
331 Egt2p. In contrast, Hara et al. (2012) efficiently localized a GPCR-specific peptide ligand to the

plasma membrane by fusing it with the minimum length (six amino acids including the ω site) of the membrane-associated GPI protein Yps1p and activated the yeast pheromone response pathway. To our knowledge, however, no comparative study on the final anchorage position of GPI-attached proteins liberated from the yeast plasma membrane has been reported.

In this study, we investigated the effect of the fusion of GPI-anchoring domains to heterologous proteins on their localization in yeast cells using two GPI-anchoring domains derived from well-characterized GPI-CWPs, namely Sed1p and Sag1p (Supplementary Fig. S1). As the Sed1- and Sag1-anchoring domains used in this study have hydrophobic amino acids in their ω-minus region and the serine and threonine contents are high (41.8 and 40.3%, respectively), the proteins fused with these domains were expected to be predominantly localized to the cell wall. Confocal microscopy observations using a reporter protein (eGFP) indicated that fusing the GPI-anchoring domain to eGFP promotes intracellular transportation efficiency of the fusion protein. This result is in good agreement with the results of cell-surface BGL activity measurements in a previous study (Inokuma et al., 2014). Similar anchoring domain-dependent changes in the intracellular accumulation of GPI-attached proteins were also reported in the methylotrophic yeast *Pichia pastoris* (Zhang et al., 2013). Furthermore, immunoelectron-microscopic analysis of ultra-thin sections of the eGFP-displaying yeast cells clearly indicated that the fusion of GPI-anchoring domains with eGFP also determined its final immobilized location, and in particular, the depth in the cell wall. To our knowledge, this is the first report comparing the final destination of a heterologous protein fused with different GPI-anchoring domains in the yeast cell wall. Immunoelectron-microscopic analyses of yeast cells displaying enzymes (glucoamylase and carboxymethylcellulase) fused with the Sag1-anchoring domain have been reported previously (Murai et al., 1997a; Murai et al., 1997b). In these reports, the fusion proteins were detected only on the external surface of the cell wall. These results are not consistent with our observation shown in Fig. 2B, which is likely due to a difference in the analytical methods adopted. In the current study,

357 immunostaining was carried out after the embedding and ultrathin sectioning of the cells (see
358 Materials and Methods section), whereas in previous reports, immunostaining was performed prior
359 to embedding and sectioning (Murai et al., 1997a; Murai et al., 1997b). Therefore, enzymes fused
360 with the Sag1-anchoring domain buried in the glucan layer might not have been detected in these
361 previous reports.

362 The results presented in this study suggest that yeast cells recognize GPI-anchoring domains
363 attached to target proteins and control their anchorage positions in the cell wall. Although the
364 anchorage mechanism of yeast GPI-CWPs liberated from the plasma membrane to the cell wall
365 remains unclear, recent studies have suggested that plasma membrane-anchored GPI proteins
366 Dfg5p and Dcw1p are potential candidates for cross-linking the GPI-anchor remnant and cell wall
367 β-(1 to 6) glucan (Gonzalez et al., 2010; Orlean, 2012). These proteins are putative
368 glycosidase/transglycosidases homologous to bacterial family 75 (Cantarel et al., 2009) and
369 depletion of these enzymes by repressing their expression in the double-null background led to
370 secretion of a GPI-CWP into the medium (Kitagaki et al., 2002). These enzymes might recognize
371 differences in GPI anchoring domains and be involved in controlling the anchorage position of
372 GPI-attached proteins. Further analysis using GPI-anchoring domains derived from other GPI-
373 CWPs are urgently required to identify the determinants of the anchorage position of GPI-attached
374 proteins. On the other hand, in order to expand this research to a wide range of GPI-CWPs, it will
375 be necessary to develop a novel method for high-throughput anchorage position analysis.

376 In this study, we also demonstrated the application of the localization control technique for the
377 construction of cellulase-displaying yeast. EGII, which requires contact with bulky insoluble
378 cellulose, was preferentially localized to the external surface of the cell wall by fusing it with the
379 Sed1-anchoring domain. Concomitantly, BGL1 was immobilized on the inside of the cell wall
380 using the Sag1-anchoring domain, which avoided competition with EGII for space on the outer
381 surface. As a result of the reallocation of cell wall space, cell-surface EG activity in BY-ESBA

382 (containing combinations of EGII-Sed1 + BGL1-Sag1) was almost twice that of BY-ESBS
383 (containing combinations of EGII-Sed1 + BGL1-Sed1) (Fig. 3A). Despite lower BGL1 activity
384 (Fig. 3A), BY-ESBA achieved a higher ethanol titer after the simultaneous saccharification and
385 fermentation of pretreated lignocellulosic biomass, as compared to that with BY-ESBS (Fig. 4);
386 this is likely due to the enhanced access of EGII to its polymeric substrate. These results indicate
387 the importance of the anchorage position control of target proteins in yeast cell-surface display
388 systems.

389 To investigate the status of cellulases immobilized in the yeast cell wall in more detail, we
390 performed relative quantitative analysis of cell wall-associated cellulases in BY-ESBS and BY-
391 ESBA strains by nano-UPLC-MS^E. The amount of cell wall-associated BGL1 per unit dry cell-
392 weight of BY-ESBS was 1.67-fold higher compared to that with BY-ESBA. This result indicates
393 that the difference in cell-surface BGL activity between these strains is due to differences in the
394 abundance of cell wall-associated BGL1. Although we attempted the relative quantification of cell
395 wall-associated EGII, this protein was not detected in the cell wall fractions of both strains. One
396 possible reason for this result could be the hyperglycosylation of EGII in *S. cerevisiae*. It was
397 previously reported that recombinant *T. reesei* EGII expressed in *S. cerevisiae* has a larger
398 molecular mass compared to the native enzyme produced by *T. reesei* (48 kDa) due to different
399 levels of glycosylation; moreover, a portion of recombinant EGII presents as hyperglycosylated
400 isoforms with a broad molecular mass up to 200 kDa (Qin et al., 2008). In contrast, it was reported
401 that the glycosylation level of recombinant *Aspergillus kawachii* BGLA (Genbank annotation No.
402 BAA19913), which has significant similarity (81.8%) to *A. aculeatus* BGL1 (Genbank annotation
403 No. BAA10968) produced by *S. cerevisiae*, is fairly homogenous and that this protein has an
404 apparent molecular mass of 120 kDa (Iwashita et al., 1999). In the nano-UPLC-MS^E analysis,
405 protein identification is conducted based on precise mass measurements of tryptic peptides from
406 each protein. The masses of tryptic peptides derived from EGII displayed in this study might have

been altered by variable glycosylation, and therefore, it might not have been possible to identify this enzyme by the nano-UPLC-MS^E analysis.

In this study, we used EG and BGL co-displaying strains for the simultaneous saccharification and fermentation of pretreated rice straw. It has been demonstrated that synergistic cooperation of EG and cellobiohydrolases (CBHs) is essential for efficient degradation of insoluble cellulose (Jalak et al. 2012). CBHs are chain end-specific processive exo-glucanases. EG randomly hydrolyzes amorphous regions of insoluble cellulose and generates reducing and non-reducing ends that can be attacked by CBHs, while CBHs recognize the cellulose chain ends and continuously hydrolyze crystalline regions between the amorphous parts into cellobiose units (Jalak et al. 2012). Previously, we reported a simultaneous saccharification and fermentation from pretreated rice straw using a recombinant yeast strain, in which BGL1, EGII, and CBHs (CBH1 and CBH2) were displayed using the Sed1-anchoring domain (Liu et al., 2016). Although direct comparison with the result shown in Fig. 4 is not possible due to differences in fermentation scale and agitation procedure, the BGL, EG, and CBHs co-displaying strain achieved approximately 9.5 g/L of ethanol production after 96 h fermentation with 0.2 FPU/g biomass of commercial cellulase cocktail (Liu et al., 2016). This ethanol titer is higher than that of BY-ESBS strain with 0.4 FPU/g biomass of commercial cellulase cocktail (7.3 g/L at 96 h, Fig. 4). These results also suggest the importance of co-display of BGL, EG, and CBHs for efficient hydrolysis of insoluble cellulosic materials. Additional display of CBHs on the cell surface of BY-ESBA strain will be required for further improvement of its ethanol yield from pretreated biomass. Furthermore, it will be necessary to verify the optimal anchorage position for CBHs in the cell wall to maximize synergies between cellulases.

The anchorage position control technique demonstrated in this study will also benefit applications of yeast cell-surface display other than the construction of cellulase-displaying yeast. The hydrolysis efficiency of other plant-derived polysaccharides such as hemicellulase and starch

may be improved by this technique because the complete hydrolysis of these polysaccharides also requires the cooperation of endo- and exo-type enzymes. In addition, the Sed1-anchoring domain that can expose the target protein to the external surface of the cell wall will also be a potential anchor candidate for protein screening requiring contact with large ligands.

5. Conclusions

In the present study, we provide the first experimental evidence that the anchorage position of GPI-attached heterologous proteins in the yeast cell wall can be controlled by the specific anchoring domain fused to them. A reporter protein (eGFP) was predominantly localized to the external surface of the cell wall when fused with the Sed1-anchoring domain, whereas the anchorage position of eGFP fused with the Sag1-anchoring domain was mainly inside of the cell wall. By applying this anchorage position control technique, the cellulolytic ability of the recombinant yeast strain co-displaying EG and BGL was successfully improved. Although further analyses using GPI-anchoring domains derived from a wide-range of GPI-CWPs are required to identify the determinants of GPI-attached protein anchorage positions, our novel strategy for anchorage position control will enable the efficient utilization of the cell wall space for various fields of yeast cell-surface display.

Declaration of interest

The authors declare that they have no competing interests.

Acknowledgements

This work was supported in part by a Special Coordination Fund for Promoting Science and Technology, Creation of Innovative Centers for Advanced Interdisciplinary Research Areas (Innovative BioProduction Kobe) from the Ministry of Education, Culture, Sports, Science and

457 Technology (MEXT), Japan Society for the Promotion of Science (JSPS) KAKENHI Grant
458 Number JP18K05554, and JSPS and National Research Foundation (NRF) of South Africa under
459 the JSPS - NRF Joint Research Program (NRF Grant Number 118894).
460

461 **References**

462 Andreu, C., Del Olmo, M.L., 2018. Yeast arming systems: pros and cons of different protein
463 anchors and other elements required for display. Appl Microbiol Biotechnol. 102, 2543-
464 2561. https://doi.org/10.1007/s00253-018-8827-6.

465 Angelini, A., Chen, T.F., de Picciotto, S., Yang, N.J., Tzeng, A., Santos, M.S., Van Deventer, J.A.,
466 Traxlmayr, M.W., Wittrup, K.D., 2015. Protein Engineering and Selection Using Yeast
467 Surface Display. Methods Mol Biol. 1319, 3-36. https://doi.org/10.1007/978-1-4939-
468 2748-7_1.

469 Bamba, T., Inokuma, K., Hasunuma, T., Kondo, A., 2018. Enhanced cell-surface display of a
470 heterologous protein using *SED1* anchoring system in *SED1*-disrupted *Saccharomyces*
471 *cerevisiae* strain. J Biosci Bioeng. 125, 306-310.
472 https://doi.org/10.1016/j.jbiosc.2017.09.013.

473 Cantarel, B.L., Coutinho, P.M., Rancurel, C., Bernard, T., Lombard, V., Henrissat, B., 2009. The
474 Carbohydrate-Active EnZymes database (CAZy): an expert resource for Glycogenomics.
475 Nucleic Acids Res. 37, D233-D238. https://doi.org/10.1093/nar/gkn663.

476 Chen, D.C., Yang, B.C., Kuo, T.T., 1992. One-step transformation of yeast in stationary phase.
477 Curr Genet. 21, 83- 84.

478 Decker, C.H., Visser, J., Schreier, P., 2000. β-glucosidases from five black *Aspergillus* species:
479 study of their physico-chemical and biocatalytic properties. J Agric Food Chem. 48,
480 4929-4936. https://doi.org/10.1021/jf000434d

481 Doering, T.L., Schekman, R., 1996. GPI anchor attachment is required for Gas1p transport from
482 the endoplasmic reticulum in COP II vesicles. EMBO J. 15, 182-191.
483 Dupres, V., Dufrêne, Y.F., Heinisch, J.J., 2010. Measuring cell wall thickness in living yeast cells
484 using single molecular rulers. ACS Nano. 4, 5498-5504.
485 https://doi.org/10.1021/nn101598v.
486 Frieman, M.B., Cormack, B.P., 2003. The omega-site sequence of glycosylphosphatidylinositol-
487 anchored proteins in *Saccharomyces cerevisiae* can determine distribution between the
488 membrane and the cell wall. Mol Microbiol. 50, 883-896.
489 Frieman, M.B., Cormack, B.P., 2004. Multiple sequence signals determine the distribution of
490 glycosylphosphatidylinositol proteins between the plasma membrane and cell wall in
491 *Saccharomyces cerevisiae*. Microbiology. 150, 3105-3114.
492 https://doi.org/10.1099/mic.0.27420-0.
493 Gonzalez, M., Goddard, N., Hicks, C., Ovalle, R., Rauceo, J.M., Jue, C.K., Lipke, P.N., 2010. A
494 screen for deficiencies in GPI-anchorage of wall glycoproteins in yeast. Yeast. 27, 583-
495 596. https://doi.org/10.1002/yea.1797.
496 Grzeschik, J., Hinz, S. C., Könning, D., Pirzer, T., Becker, S., Zielonka, S., Kolmar, H., 2017. A
497 simplified procedure for antibody engineering by yeast surface display: Coupling display
498 levels and target binding by ribosomal skipping. Biotechnol J. 12.
499 https://doi.org/10.1002/biot.201600454.
500 Hamada, K., Terashima, H., Arisawa, M., Yabuki, N., Kitada, K., 1999. Amino acid residues in the
501 omega-minus region participate in cellular localization of yeast
502 glycosylphosphatidylinositol-attached proteins. J Bacteriol. 181, 3886-3889.
503 Hara, K., Ono, T., Kuroda, K., Ueda, M., 2012. Membrane-displayed peptide ligand activates the
504 pheromone response pathway in *Saccharomyces cerevisiae*. J Biochem. 151, 551-557.
505 https://doi.org/10.1093/jb/mvs027.

506 Hasunuma, T., Sung, K., Sanda, T., Yoshimura, K., Matsuda, F., Kondo, A., 2011. Efficient
507 fermentation of xylose to ethanol at high formic acid concentrations by metabolically
508 engineered *Saccharomyces cerevisiae*. Appl Microbiol Biot. 90, 997-1004.
509 https://doi.org/10.1007/s00253-011-3085-x.
510 Inokuma, K., Bamba, T., Ishii, J., Ito, Y., Hasunuma, T., Kondo, A., 2016. Enhanced cell-surface
511 display and secretory production of cellulolytic enzymes with *Saccharomyces cerevisiae*
512 Sed1 signal peptide. Biotechnol Bioeng. 113, 2358-2366.
513 https://doi.org/10.1002/bit.26008.
514 Inokuma, K., Hasunuma, T., Kondo, A., 2014. Efficient yeast cell-surface display of exo- and
515 endo-cellulase using the *SED1* anchoring region and its original promoter. Biotechnol
516 Biofuels. 7, 8. https://doi.org/10.1186/1754-6834-7-8.
517 Inokuma, K., Hasunuma, T., Kondo, A., 2018. Whole cell biocatalysts using enzymes displayed on
518 yeast cell surface. In: Chang, H., (Ed.), Emerging Areas in Bioengineering. Wiley-VCH,
519 pp. 81-92.
520 Iwashita, K., Nagahara, T., Kimura, H., Takano, M., Shimoi, H., Ito, K., 1999. The *bglA* gene of
521 *Aspergillus kawachii* encodes both extracellular and cell wall-bound β-glucosidases.
522 Appl Environ Microbiol. 65, 5546-5553.
523 Jalak, J., Kurašin, M., Teugjas, H., Väljamäe, P., 2012. Endo-exo synergism in cellulose hydrolysis
524 revisited. J Biol Chem. 287, 28802-28815. https://doi.org/10.1074/jbc.M112.381624.
525 Kitagaki, H., Wu, H., Shimoi, H., Ito, K., 2002. Two homologous genes, *DCW1* (YKL046c) and
526 *DFG5*, are essential for cell growth and encode glycosylphosphatidylinositol (GPI)-
527 anchored membrane proteins required for cell wall biogenesis in *Saccharomyces*
528 *cerevisiae*. Mol Microbiol. 46, 1011-1022.
529 Klis, F.M., Caro, L.H.P., Vossen, J.H., Kapteyn, J.C., Ram, A.F.J., Montijn, R.C., VanBerkel,
530 M.A.A., VandenEnde, H., 1997. Identification and characterization of a major building

block in the cell wall of *Saccharomyces cerevisiae*. Biochem Soc Trans. 25, 856-860. https://doi.org/10.1042/bst0250856.

Li, B., Scarselli, M., Knudsen, C.D., Kim, S.K., Jacobson, K.A., McMillin, S.M., Wess, J., 2007. Rapid identification of functionally critical amino acids in a G protein-coupled receptor. Nat Methods. 4, 169-174. https://doi.org/10.1038/nmeth990.

Liu, Z., Ho, S.H., Hasunuma, T., Chang, J.S., Ren, N.Q., Kondo, A., 2016. Recent advances in yeast cell-surface display technologies for waste biorefineries. Bioresour Technol. 215, 324-333. https://doi.org/10.1016/j.biortech.2016.03.132.

Liu, Z., Inokuma, K., Ho, S.H., den Haan, R., van Zyl, W.H., Hasunuma, T., Kondo, A., 2017. Improvement of ethanol production from crystalline cellulose via optimizing cellulase ratios in cellulolytic *Saccharomyces cerevisiae*. Biotechnol Bioeng. 114, 1201-1207. https://doi.org/10.1002/bit.26252.

Lu, C.F., Kurjan, J., Lipke, P.N., 1994. A pathway for cell wall anchorage of *Saccharomyces cerevisiae* alpha-agglutinin. Mol Cell Biol. 14, 4825-4833. https://doi.org/10.1128/MCB.14.7.4825.

Matano, Y., Hasunuma, T., Kondo, A., 2012. Display of cellulases on the cell surface of *Saccharomyces cerevisiae* for high yield ethanol production from high-solid lignocellulosic biomass. Bioresour Technol. 108, 128-133. https://doi.org/10.1016/j.biortech.2011.12.144.

Murai, T., Ueda, M., Atomi, H., Shibasaki, Y., Kamasawa, N., Osumi, M., Kawaguchi, T., Arai, M., Tanaka, A., 1997a. Genetic immobilization of cellulase on the cell surface of *Saccharomyces cerevisiae*. Appl Microbiol Biotechnol. 48, 499-503.

Murai, T., Ueda, M., Yamamura, M., Atomi, H., Shibasaki, Y., Kamasawa, N., Osumi, M., Amachi, T., Tanaka, A., 1997b. Construction of a starch-utilizing yeast by cell surface engineering. Appl Environ Microbiol. 63, 1362-1366.

556 Nuoffer, C., Jeno, P., Conzelmann, A., Riezman, H., 1991. Determinants for glycophospholipid
557 anchoring of the *Saccharomyces cerevisiae* GAS1 protein to the plasma membrane. Mol
558 Cell Biol. 11, 27-37. https://doi.org/10.1128/mcb.11.1.27.
559 Orlean, P., 2012. Architecture and biosynthesis of the *Saccharomyces cerevisiae* cell wall. Genetics.
560 192, 775-818. https://doi.org/10.1534/genetics.112.144485.
561 Qin, Y., Wei, X., Liu, X., Wang, T., Qu, Y., 2008. Purification and characterization of recombinant
562 endoglucanase of *Trichoderma reesei* expressed in *Saccharomyces cerevisiae* with
563 higher glycosylation and stability. Protein expr and purif. 58, 162-167.
564 https://doi.org/10.1016/j.pep.2007.09.004.
565 Richins, R.D., Kaneva, I., Mulchandani, A., Chen, W., 1997. Biodegradation of organophosphorus
566 pesticides by surface-expressed organophosphorus hydrolase. Nat Biotechnol. 15, 984-
567 987. https://doi.org/10.1038/nbt1097-984.
568 Sasaki, K., Tsuge, Y., Sasaki, D., Teramura, H., Inokuma, K., Hasunuma, T., Ogino, C., Kondo, A.,
569 2015. Mechanical milling and membrane separation for increased ethanol production
570 during simultaneous saccharification and co-fermentation of rice straw by xylose-
571 fermenting *Saccharomyces cerevisiae*. Bioresour Technol. 185, 263-268.
572 https://doi.org/10.1016/j.biortech.2015.02.117.
573 Shibasaki, S., Kawabata, A., Tanino, T., Kondo, A., Ueda, M., Tanaka, M., 2009. Evaluation of the
574 biodegradability of polyurethane and its derivatives by using lipase-displaying arming
575 yeast. Biocontrol Sci. 14, 171-175.
576 Shibasaki, S., Ueda, M., 2014. Bioadsorption strategies with yeast molecular display technology.
577 Biocontrol Sci. 19, 157-164. https://doi.org/10.4265/bio.19.157.
578 Tang, X., Liang, B., Yi, T., Manco, G., Palchetti, I., Liu, A., 2014. Cell surface display of
579 organophosphorus hydrolase for sensitive spectrophotometric detection of *p*-nitrophenol

substituted organophosphates. Enzyme Microb Technol. 55, 107-112. https://doi.org/10.1016/j.enzmictec.2013.10.006.

Terashima, H., Hamada, K., Kitada, K., 2003. The localization change of Ybr078w/Ecm33, a yeast GPI-associated protein, from the plasma membrane to the cell wall, affecting the cellular function. FEMS Microbiol Lett. 218, 175-180. https://doi.org/10.1111/j.1574-6968.2003.tb11515.x.

Trudeau, D.L., Lee, T.M., Arnold, F.H., 2014. Engineered thermostable fungal cellulases exhibit efficient synergistic cellulose hydrolysis at elevated temperatures. Biotechnol Bioeng. 111, 2390-2397. https://doi.org/10.1002/bit.25308.

Van der Vaart, J.M., te Biesebeke, R., Chapman, J.W., Toschka, H.Y., Klis, F.M., Verrips, C.T., 1997. Comparison of cell wall proteins of *Saccharomyces cerevisiae* as anchors for cell surface expression of heterologous proteins. Appl Environ Microbiol. 63, 615-620.

Wang, H., Lang, Q., Li, L., Liang, B., Tang, X., Kong, L., Mascini, M., Liu, A., 2013. Yeast surface displaying glucose oxidase as whole-cell biocatalyst: construction, characterization, and its electrochemical glucose sensing application. Anal Chem. 85, 6107-6112. https://doi.org/10.1021/ac400979r.

Zhang, L., Liang, S., Zhou, X., Jin, Z., Jiang, F., Han, S., Zheng, S., Lin, Y., 2013. Screening for glycosylphosphatidylinositol-modified cell wall proteins in *Pichia pastoris* and their recombinant expression on the cell surface. Appl Environ Microbiol. 79, 5519-5526. https://doi.org/10.1128/AEM.00824-13.

605 **Table 1** Characteristics of yeast strains used in this study

Strains	Relevant genotype	Source
S. cerevisiae BY4741	*MAT**a** his3Δ1 leu2Δ0 met15Δ0 ura3Δ0*	Invitrogen
BY-eGFP-SSS	BY4741/pIeGFP-SSS	This study
BY-eGFP-SSA	BY4741/pIeGFP-SSA	This study
BY-eGFP-SSn	BY4741/pIeGFP-SS2	This study
BY-BG-SSS	BY4741/pIBG-SSS	Inokuma et al. (2016)
BY-EG-SSS	BY4741/pIEG-SSS	Inokuma et al. (2016)
BY-ESBS	BY-EG-SSS/pIL2BG-SSS	This study
BY-ESBA	BY-EG-SSS/pIL2BG-SSA	This study

606

607

608 **Figure legends**

609

610 **Fig. 1** Schematic summary of the construction of gene cassettes used in this study. **(A)** Gene
611 cassettes for cell-surface display and the secretory production of eGFP. **(B)** Gene cassettes for the
612 cell-surface display of BGL1. **(C)** Gene cassettes for cell-surface display of EGII.

613

614 **Fig. 2** Localization analyses of eGFP fused with Sed1- or Sag1-anchoring domains. **(A)**
615 Fluorescence images of strains BY-eGFP-SSS, BY-eGFP-SSA, and BY-eGFP-SSn. The cells
616 were incubated in YPD medium for 48 h, stained with FM4-64 (red) to visualize vacuolar
617 membranes, and then observed using a confocal microscope. **(B)** Immunoelectron micrographs of
618 strains BY-eGFP-SSS and BY-eGFP-SSA. The cells were immunogold-labeled with an antibody
619 against GFP. The arrowheads indicate gold particles.

620

621 **Fig. 3** Effects of anchorage position control on enzyme activities of cellulase-displaying yeasts. **(A)**
622 Comparison of cell-surface EG and BGL activities in strains BY-BG-SSS, BY-ESBS, and BY-
623 ESBA after cultivation in YPD medium for 48 h. The relative EG activity of each strain is shown
624 as a fold-change in EG activity relative to the average level observed with the parental strain BY-
625 EG-SSS. **(B)** Comparison of transcript levels of EGII- and BGL1-encoding genes in strains BY-
626 ESBS and BY-ESBA after cultivation in YPD medium for 48 h. The relative transcript level of
627 each gene is shown as a fold-change in mRNA levels relative to the average level detected in strain
628 BY-ESBS. **(C)** Relative quantification of BGL1 in the cell walls of strains BY-ESBS and BY-
629 ESBA by nanoscale ultra-pressure liquid chromatography electrospray ionization quadrupole time-
630 of-flight tandem mass spectrometry (nano-UPLC-MS^E). The amount of BGL1 was normalized to
631 the dry cell weight of each strain. Data are presented as the means ± standard deviation (n = 3).

632

Fig. 4 Time course of the simultaneous saccharification and fermentation of 100 g dry weight/L of pretreated rice straw by strains BY-ESBS, BY-ESBA, and their parental strain (BY4741). A small amount of a commercial cellulase cocktail (0.4 FPU/g-biomass) was added to the fermentation mixture. Data are presented as the means ± standard deviation (n = 3).

641 **Supplementary materials**

642 **Text S1** Plasmid construction and yeast transformation.

643

644 **Table S1** Characteristics of integrative plasmids used in this study.

645

646 **Table S2** PCR primers used in this study.

647

648 **Fig. S1** Amino acid sequence of Sed1- and Sag1-anchoring domains used in this study. The C-
649 terminal GPI attachment site (the ω site) was marked in bold. The hydrophobic amino acid residues
650 in the ω-minus region are underlined.

651

Graphical abstract

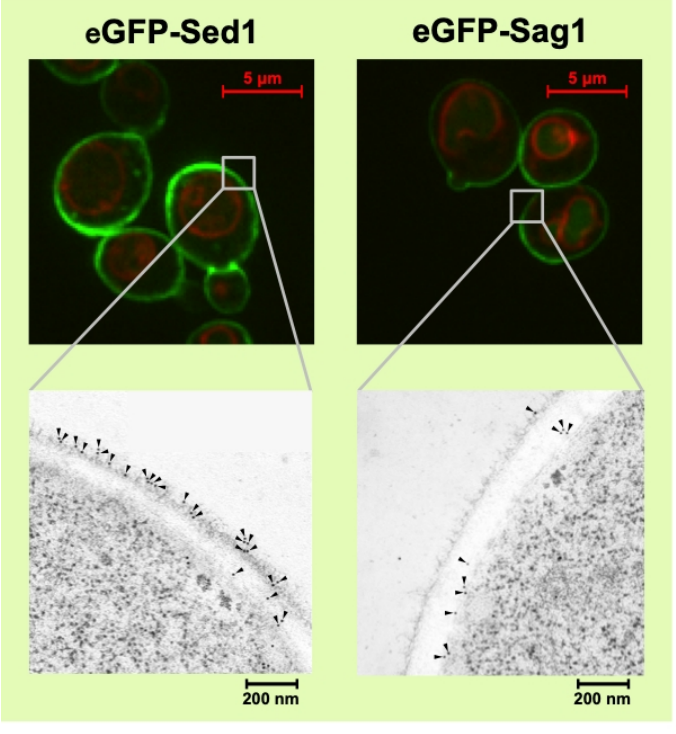

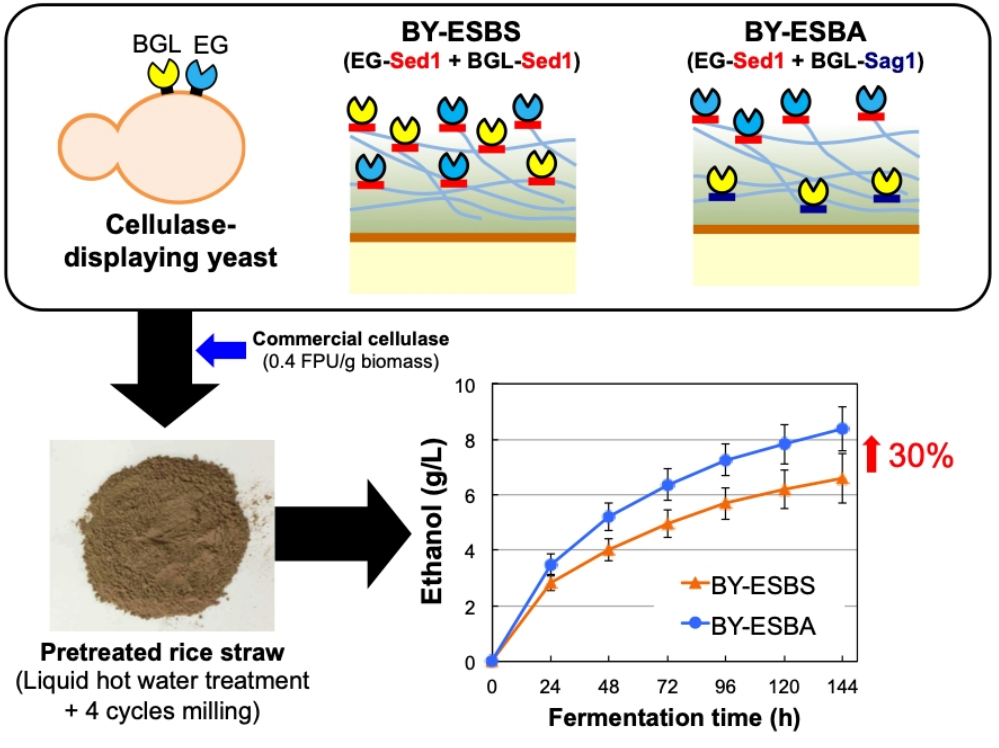

Fig. 1

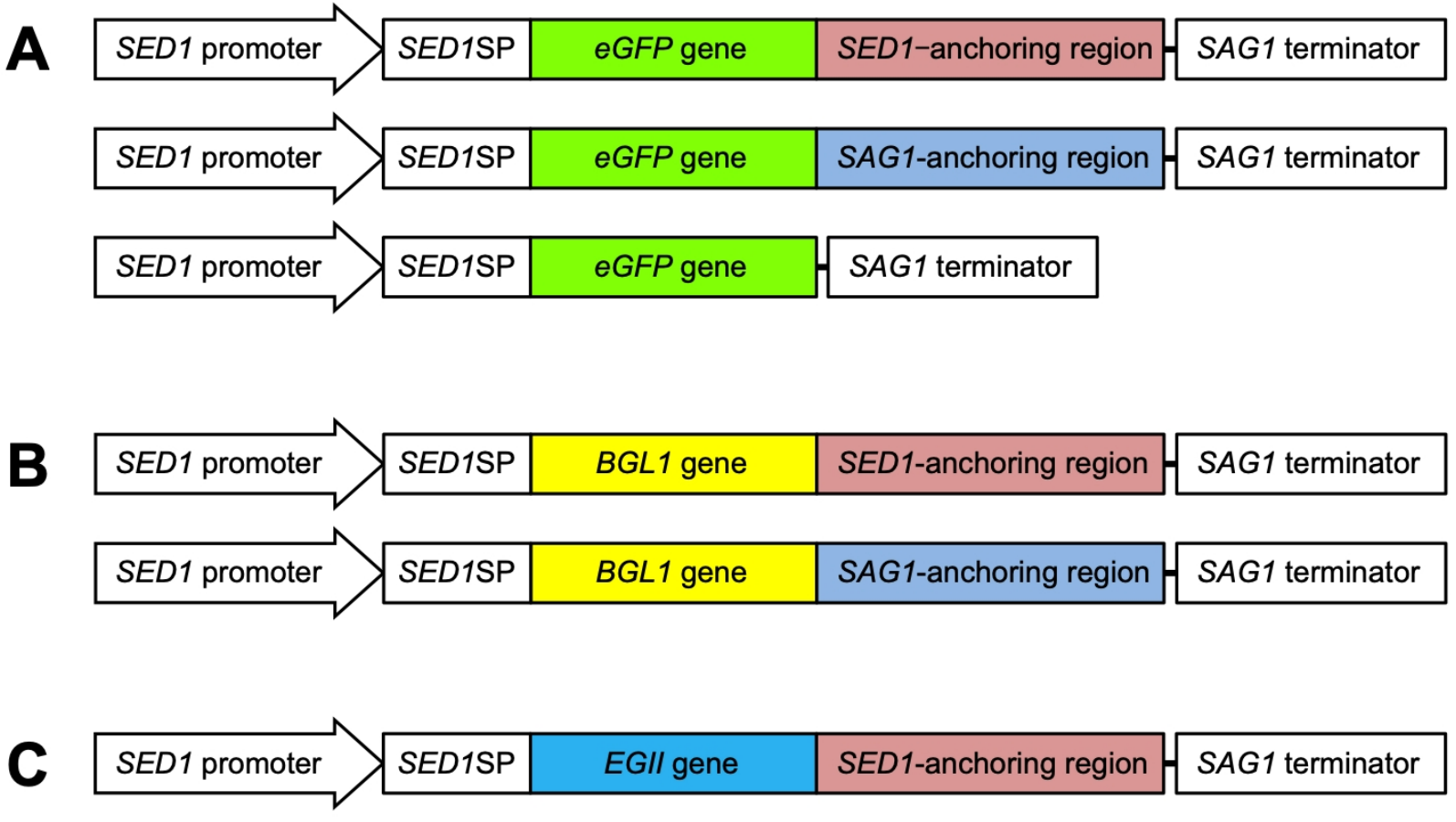
A
SED1 promoter
SED1SP
eGFP gene
SED1−anchoring region
SAG1 terminator
SED1 promoter
SED1SP
eGFP gene
SAG1-anchoring region
SAG1 terminator
SED1 promoter
SED1SP
eGFP gene
SAG1 terminator
B
SED1 promoter
SED1SP
BGL1 gene
SED1-anchoring region
SAG1 terminator
SED1 promoter
SED1SP
BGL1 gene
SAG1-anchoring region
SAG1 terminator
C
SED1 promoter
SED1SP
EGII gene
SED1-anchoring region
SAG1 terminator

Fig. 2

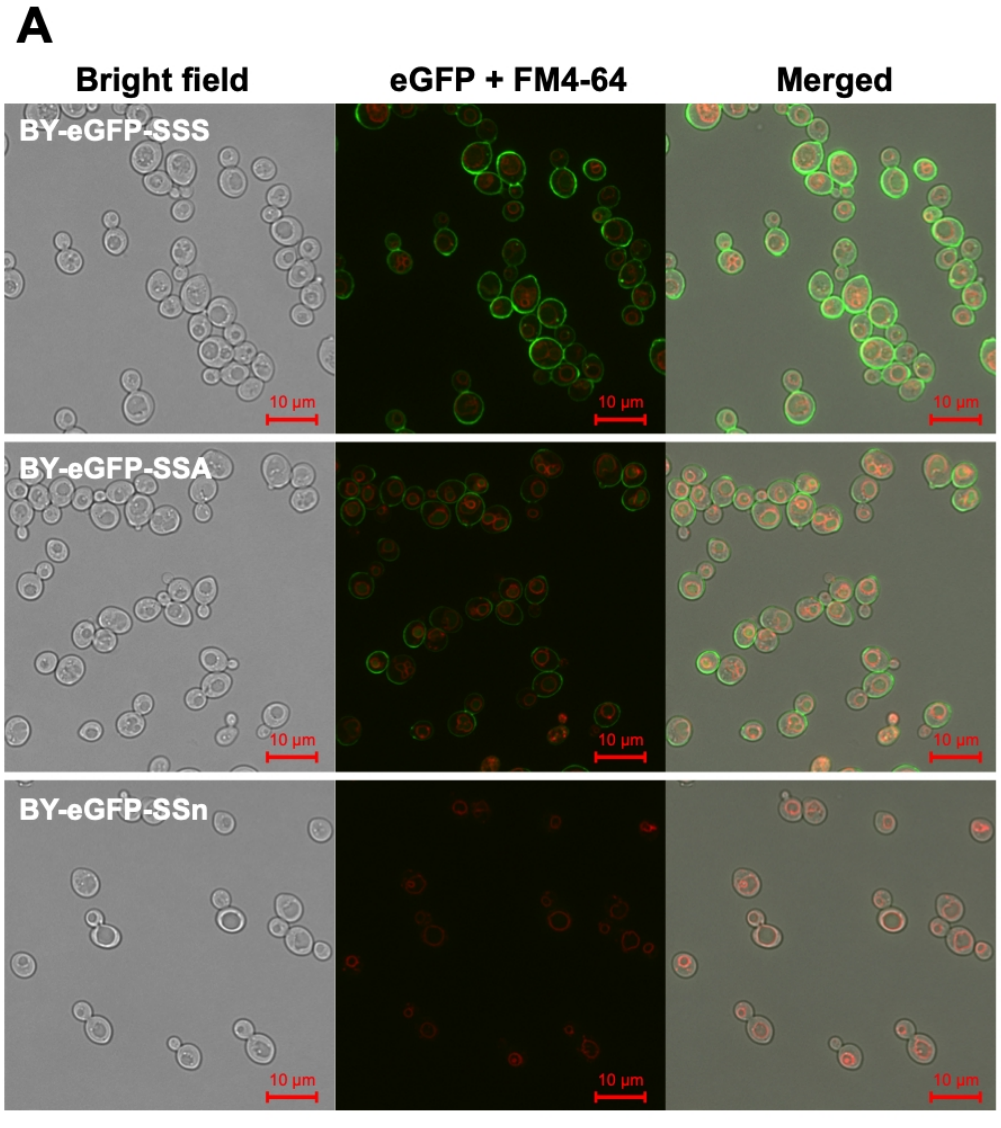
A
Bright field
eGFP + FM4-64
Merged
BY-eGFP-SSS
BY-eGFP-SSA
BY-eGFP-SSn
10 μm

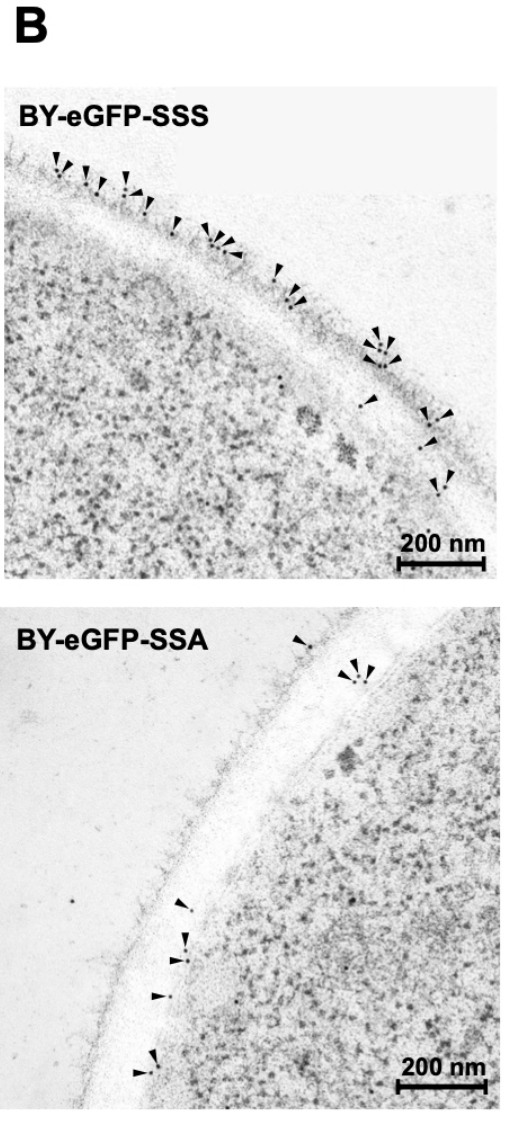
B
BY-eGFP-SSS
200 nm
BY-eGFP-SSA
200 nm

Fig. 3

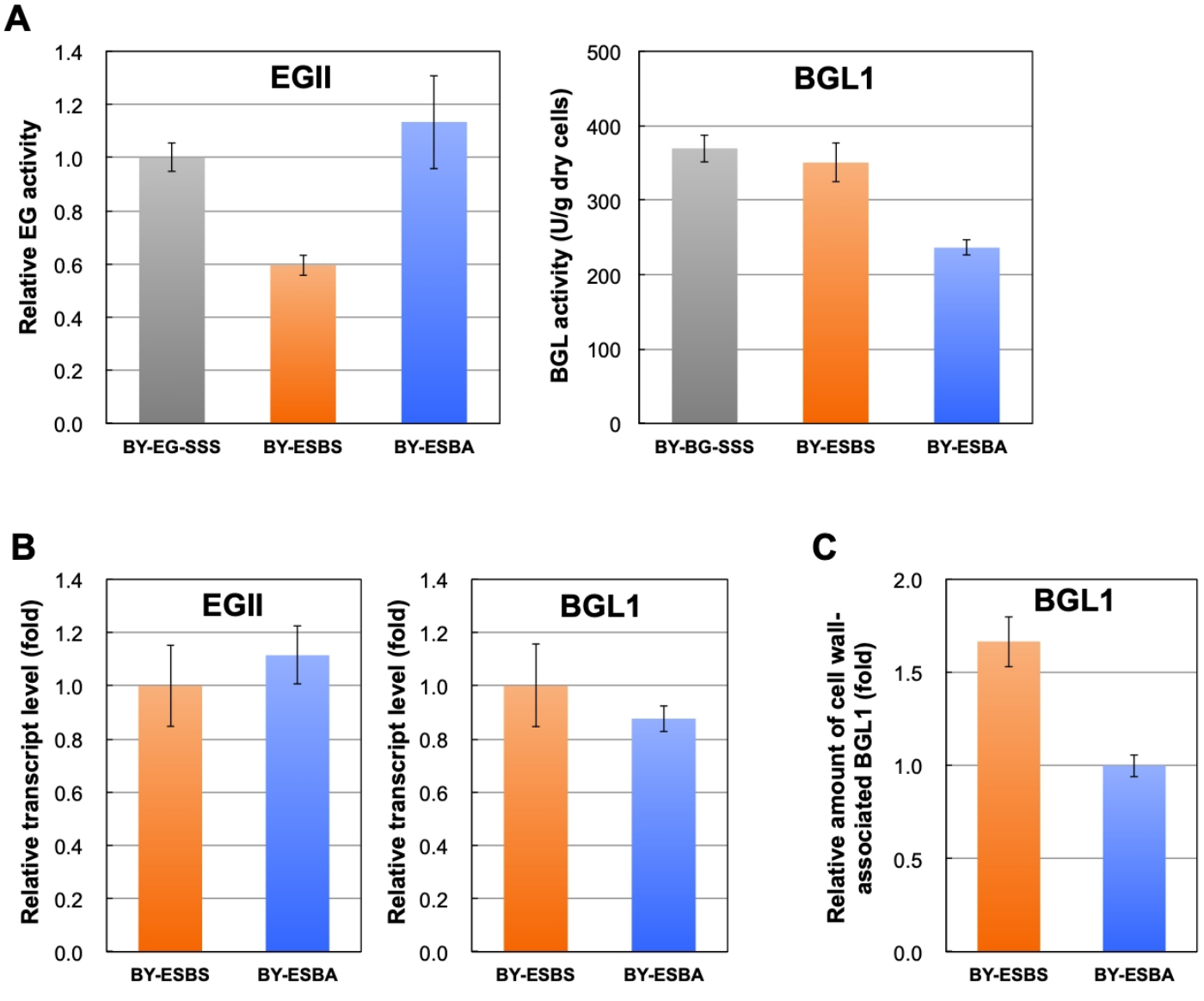
A
EGII
Relative EG activity
1.4
1.2
1.0
0.8
0.6
0.4
0.2
0.0
BY-EG-SSS
BY-ESBS
BY-ESBA
BGL1
BGL activity (U/g dry cells)
500
400
300
200
100
0
BY-BG-SSS
BY-ESBS
BY-ESBA
B
EGII
Relative transcript level (fold)
BY-ESBS
BY-ESBA
BGL1
Relative transcript level (fold)
BY-ESBS
BY-ESBA
C
BGL1
Relative amount of cell wall-associated BGL1 (fold)
2.0
1.5
1.0
0.5
0.0
BY-ESBS
BY-ESBA

Fig. 4

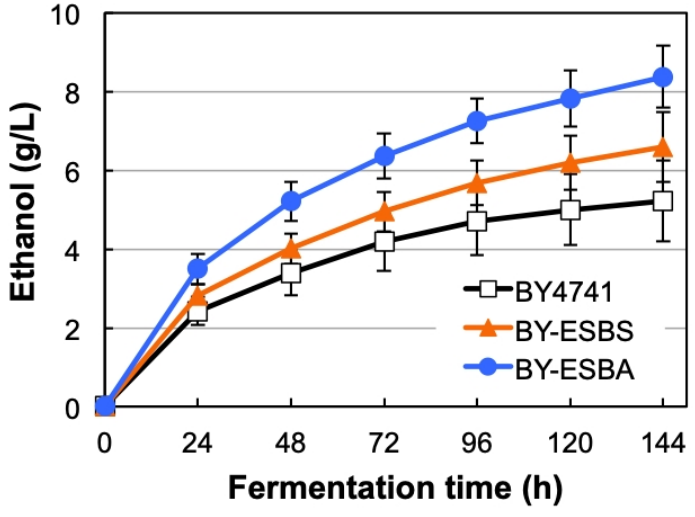
Ethanol (g/L)
10
8
6
4
2
0
0
24
48
72
96
120
144
Fermentation time (h)
BY4741
BY-ESBS
BY-ESBA

Supplementary materials

Novel strategy for anchorage position control of GPI-attached proteins in the yeast cell wall using different GPI-anchoring domains

Kentaro Inokuma,[a] Hiroki Kurono,[a] Riaan den Haan,[b] Willem Heber van Zyl,[c] Tomohisa Hasunuma,[a,d,*] Akihiko Kondo[a,d,e,*]

[a] Graduate School of Science, Technology and Innovation, Kobe University, 1-1 Rokkodai-cho, Nada-ku, Kobe 657-8501, Japan

[b] Department of Biotechnology, University of the Western Cape, Bellville, 7530, South Africa

[c] Department of Microbiology, Stellenbosch University, Private Bag X1, Matieland, 7602, South Africa

[d] Engineering Biology Research Center, Kobe University, 1-1 Rokkodai-cho, Nada-ku, Kobe 657-8501, Japan

[e] Biomass Engineering Program, RIKEN, 1-7-22 Suehiro-cho, Tsurumi-ku, Yokohama, Kanagawa 230-0045, Japan

* Corresponding authors:

Tomohisa Hasunuma

Telephone: +81-78-803-6356, Fax: +81-78-803-6362

E-mail: hasunuma@port.kobe-u.ac.jp

Akihiko Kondo

Telephone: +81-78-803-6196, Fax: +81-78-803-6196

E-mail: akondo@kobe-u.ac.jp

Text S1 Plasmid construction and yeast transformation

The plasmids and primers used in this study are listed in supplemental data Tables S1 and S2, respectively. The plasmids for cell-surface display of the enhanced green fluorescent protein (eGFP) using Sed1-anchoring domain were constructed based on the plasmid pIEG-SS (Inokuma et al., 2014) containing the sequences for the *S. cerevisiae SED1* promoter, the signal peptide (SP) sequence derived from *Rhizopus oryzae* glucoamylase (*GLUA*SP), *Trichoderma reesei EGII*, *S. cerevisiae SED1*-anchoring region, and *SAG1* terminator as follows: Inverse PCR with the SED1a-F and GLUASP-R primers was performed to replace the *EGII* of pIEG-SS to *eGFP*. The DNA fragment encoding the *eGFP* was amplified from pGK426EGFP (Ishii et al., 2009) by PCR using the eGFP-F1 and eGFP- R1 primers. These fragments were ligated by the isothermal assembly method (Gibson et al., 2009), and the resulting plasmid was named pIeGFP-SGS. Then, Inverse PCR with the SAG1t-F1 and eGFP-R2 primers was performed to replace the *SED1*-anchoring region of pIeGFP-SGS to the *SAG1*-anchoring region. The DNA fragment encoding the *SAG1*-anchoring region amplified from pIEG-TA (Inokuma et al., 2014) by PCR using the SAG1a-F1 and SAG1a-R primers. These fragments were ligated by the isothermal assembly method (Gibson et al., 2009), and the resulting plasmid was named pIeGFP-SGA. Similarly, inverse PCR with the SAG1t-F2 and eGFP-R3 primers was performed to remove the *SED1*-anchoring region of pIeGFP-SGS. This fragment was self-ligated by the isothermal assembly method (Gibson et al., 2009), and the resulting plasmid was named pIeGFP-SGn. Finally, inverse PCR with the eGFP-F2 and Vector-R1 primers was performed to replace *GLUA*SP of the plasmids pIeGFP-SGS, pIeGFP-SGA, and pIeGFP-SGn to the SP sequence derived from *Saccharomyces cerevisiae SED1* (*SED1*SP). The DNA fragment encoding the *SED1* promotor *and SED1*SP was amplified from pIBG-SSS (Inokuma et al., 2016) by PCR using the SED1p-F and SED1SP-R primers. Then, the *SED1* promotor-*SED1*SP fragment was ligated the vector fragments derived from pIeGFP-SGS, pIeGFP-SGA, and pIeGFP-SGn by the isothermal assembly method (Gibson et al., 2009), respectively. The resulting plasmids were named pIeGFP-SSS, pIeGFP-SSA, and pIeGFP-SSn, respectively.

The plasmid for cell-surface display of *Aspergillus aculeatus* β-glucosidase 1 (BGL1) using Sed1-anchoring domain was constructed as follows: Inverse PCR with the Vector-F and Vector-R2 primers was performed to replace the *HIS3* of pIBG-SSS (Inokuma et al., 2016) to the I2 region (a part of the 3' noncoding region of *YFL021W* and *YFL020C* genes) and *LEU2*. The DNA fragment encoding the I2 region and *LEU2* was amplified from pIL2GA-SS (Inokuma et al., 2015) by PCR using the I2-F and Leu2-R primers. These fragments were ligated by the isothermal assembly method (Gibson et al., 2009), and the resulting plasmid was named pIL2BG-SSS. Then, Inverse PCR with the SAG1t-F1 and BGL1-R primers was performed to replace the *SED1*-anchoring region of pIL2BG-SSS to the *SAG1*-anchoring region. The DNA fragment encoding the *SAG1*-anchoring region amplified from pIBG-SA (Inokuma et al., 2014) by PCR using the SAG1a-F2 and SAG1a-R primers. These fragments were ligated by the isothermal assembly method (Gibson et al., 2009), and the resulting plasmid was named pIL2BG-SSA.

The plasmids pIeGFP-SSS, pIeGFP-SSA, and pIeGFP-SSn were digested with *Nde*I within *HIS3*. Then, the linearized plasmids were transformed into *S. cerevisiae* BY4741 by the lithium acetate method (Chen et al., 1992) and integrated into the *HIS3* locus of the chromosomal DNA by homologous recombination, respectively. The resulting strains were designated BY-eGFP-SSS, BY-eGFP-SSA, and BY-eGFP-SSn, respectively. Similarly, the plasmids pIL2BG-SSS and pIL2BG-SSA were digested with *Nde*I within I2 region. Then, the linearized plasmids were transformed into the BY-EG-SSS strain (Inokuma et al., 2016) by the lithium acetate method (Chen et al., 1992) and integrated into the I2 region of the chromosomal DNA by homologous recombination, respectively. The resulting strains were designated BY-ESBS and BY-ESBA, respectively. A single integration of each plasmid into the chromosomal DNA was verified by diagnostic PCR (colony PCR) using primers with upstream and downstream sequences of *HIS3* locus (the His3-534-F and His3-1866-R primers) and I2 region (the I2-420-F and I2-1160-R primers), respectively (data not shown).

Table S1 Characteristics of integrative plasmids used in this study.

Plasmids	Relevant genotype	Source/references
pGK426-EGFP	*URA3 PGK1*$_{P}$-*eGFP-PGK1*$_{T}$	Ishii et al. (2009)
pIeGFP-SSS	*HIS3 SED1*$_{P}$–*SED1*$_{SP}$–*eGFP*–*SED1*$_{A}$–*SAG1*$_{T}$	This study
pIeGFP-SSA	*HIS3 SED1*$_{P}$–*SED1*$_{SP}$–*eGFP*–*SAG1*$_{A}$–*SAG1*$_{T}$	This study
pIeGFP-SSn	*HIS3 SED1*$_{P}$–*SED1*$_{SP}$–*eGFP*–*SAG1*$_{T}$	This study
pIEG-SS	*HIS3 SED1*$_{P}$-*GLUA*$_{SP}$-*T. reesei EGII-SED1*$_{A}$-*SAG1*$_{T}$	Inokuma et al. (2014)
pIEG-TA	*HIS3 TDH3*$_{P}$- *GLUA*$_{SP}$-*T. reesei EGII-SAG1*$_{A}$ -*SAG1*$_{T}$	Inokuma et al. (2014)
pIBG-SS	*HIS3 SED1*$_{P}$- *GLUA*$_{SP}$-*A. aculeatus BGL1-SED1*$_{A}$-*SAG1*$_{T}$	Inokuma et al. (2014)
pIBG-SA	*HIS3 SED1*$_{P}$- *GLUA*$_{SP}$-*A. aculeatus BGL1-SAG1*$_{A}$-*SAG1*$_{T}$	Inokuma et al. (2014)
pIBG-SSS	*HIS3 SED1*$_{P}$–*SED1*$_{SP}$–*A. aculeatus BGL1*–*SED1*$_{A}$–*SAG1*$_{T}$	Inokuma et al. (2016)
pIEG-SSS	*HIS3 SED1*$_{P}$–*SED1*$_{SP}$–*T. reesei EGII*–*SED1*$_{A}$–*SAG1*$_{T}$	Inokuma et al. (2016)
pIL2GA-SS	*LEU2 SED1*$_{P}$-*GLUA*$_{SP}$-*SED1*$_{A}$-*SAG1*$_{T}$	Inokuma et al. (2015)
pIBG-SA	*HIS3 SED1*$_{P}$–*GLUA*$_{SP}$–*A. aculeatus BGL1*–*SAG1*$_{A}$–*SAG1*$_{T}$	Inokuma et al. (2014)
pIL2BG-SSS	*LEU2 SED1*$_{P}$–*SED1*$_{SP}$–*A. aculeatus BGL1*–*SED1*$_{A}$–*SAG1*$_{T}$	This study
pIL2BG-SSA	*LEU2 SED1*$_{P}$–*SED1*$_{SP}$–*A. aculeatus BGL1*–*SAG1*$_{A}$–*SAG1*$_{T}$	This study

A. aculeatus, Aspergillus aculeatus; *T. reesei, Trichoderma reesei*; *GLUA*, *Rhizopus oryzae* glucoamylase; P, promoter; SP, signal peptide sequence; A, anchoring region; T, terminator

Table S2 PCR primers used in this study.

Primers	Sequence
SED1a-F	gcatggacgagctgtacaagggctcgagtaaattatcaactgtcc
GLUASP-R	agctcctcgcccttgctcacacccatggagatctccgc
eGFP-F1	ccgcggagatctccatgggtgtgagcaagggcgagga
eGFP-R1	gttgataatttactcgagcccttgtacagctcgtccatgc
SAG1t-F1	tgctattctaaaacgggtactgtacagttagtacattgagtctaa
eGFP-R2	gagcttttggcgctcgagcccttgtacagctcgtccatgc
SAG1a-F1	gcatggacgagctgtacaagggctcgagcgccaaaa
SAG1a-R	ctcaatgtactaactgtacagtacccgttttagaatagcagg
SAG1t -F2	tggacgagctgtacaagtaaaacgggtactgtacagttagtacattgag
eGFP-R3	actgtacagtacccgttttacttgtacagctcgtccatgc
eGFP-F2	cctcgactactttggcccaagtgagcaagggcgagga
Vector-R1	gttaattttctatatccaatctggcgtaatagcgaagagg
SED1p-F	gaaatcggcaaaatccctta
SED1SP-R	agctcctcgcccttgctcacttgggccaaagtagtcgagg
Vector-F	gaaacggccttacgacgtagcggatctatgcggtgtgaaatac
Vector-R2	tgttttgacgaggtattccctatggtgcactctcagtacaatctg
I2-F	tgtactgagagtgcaccatagggaatacctcgtcaaaacaagac
Leu2-R	tttcacaccgcatagatccgctacgtcgtaaggccgtttct
BGL1-R	gttgcaccttcgggagcg
SAG1a-F2	cgtcagctgccccttcac
His3-534-F	gctttgtcttcattcaacgtttcc
His3-1866-R	cttgccacctatcaccacaactaac
I2-420-F	gaagccgcgagtacgaacaatgatg
I2-1160-R	tggtattttcgtgagcaaacccaac
rt-ACT1-F	tggattccggtgatggtgtt
rt-ACT1-R	tcaaaatggcgtgaggtagaga
rt-BGL-F	cttccagggctttgtgatgtc
rt-BGL-R	aggtgatatcgccaggcatt
rt-EG-F	ggttgtttgtctttgggtgcttac
rt-EG-R	aattgagcatttgttggaccacctt

Fig. S1 Amino acid sequence of Sed1- and Sag1-anchoring domains used in this study. The C-terminal GPI attachment site (the ω site) was marked in bold. The hydrophobic amino acid residues in the ω-minus region are underlined.

Sed1-anchoring domain (337 a. a.)

KLSTVLLSAGLASTTLAQFSNSTSASSTDVTSSSSISTSSGSVTITSSEAPESDNGTSTAAPTETS
TEAPTTAIPTNGTSTEAPTTAIPTNGTSTEAPTDTTTEAPTTALPTNGTSTEAPTDTTTEAPTTGL
PTNGTTSAFPPTTSLPPSNTTTTPPYNPSTDYTTDYTVVTEYTTYCPEPTTFTTNGKTYTVTEPTT
LTITDCPCTIEKPTTTSTTEYTVVTEYTTYCPEPTTFTTNGKTYTVTEPTTLTITDCPCTIEKSEA
PESSVPVTESKGTTTKETGVTTKQTTANPSLTVSTVVPVSSSASSHSVVINS**N**GANVVVPGALGLA
GVAMLFL*

Sag1-anchoring domain (320 a. a.)

SAKSSFISTTTTDLTSINTSAYSTGSISTVETGNRTTSEVISHVVTTSTKLSPTATTSLTIAQTSI
YSTDSYITVGTDIHTTSEVISDVETISRETASTVVAAPTSTTGWTGAMNTYISQFTSSSFATINST
PIISSSAVFETSDASIVNVHTENITNTAAVPSEEPTFVNATRNSLNSFCSSKQPSSPSSYTSSPLV
SSLSVSKTLLSTSFTPSVPTSNTYIKTKNTGYFEHTALTTSSVGLNSFSETAVSSQGTKIDTFLVS
SLIAYPSSASGSQLSGIQQNFTSTSLMISTYE**G**KASIFFSAELGSIIFLLLSYLLF*

References in the Supplemental data

Chen, D. C., Yang, B. C., Kuo, T. T., 1992. One-step transformation of yeast in stationary phase. Curr Genet. 21, 83-84.

Gibson, D. G., Young, L., Chuang, R. Y., Venter, J. C., Hutchison, C. A., 3rd, Smith, H. O., 2009. Enzymatic assembly of DNA molecules up to several hundred kilobases. Nat Methods. 6, 343-345. https://doi.org/10.1038/nmeth.1318.

Inokuma, K., Bamba, T., Ishii, J., Ito, Y., Hasunuma, T., Kondo, A., 2016. Enhanced cell-surface display and secretory production of cellulolytic enzymes with *Saccharomyces cerevisiae* Sed1 signal peptide. Biotechnol Bioeng. 113, 2358-2366. https://doi.org/10.1002/bit.26008.

Inokuma, K., Hasunuma, T., Kondo, A., 2014. Efficient yeast cell-surface display of exo- and endo-cellulase using the *SED1* anchoring region and its original promoter. Biotechnol Biofuels. 7, 8. https://doi.org/10.1186/1754-6834-7-8.

Inokuma, K., Yoshida, T., Ishii, J., Hasunuma, T., Kondo, A., 2015. Efficient co-displaying and artificial ratio control of α-amylase and glucoamylase on the yeast cell surface by using combinations of different anchoring domains. Appl Microbiol Biotechnol. 99, 1655-1663. https://doi.org/10.1007/s00253-014-6250-1.

Ishii, J., Izawa, K., Matsumura, S., Wakamura, K., Tanino, T., Tanaka, T., Ogino, C., Fukuda, H., Kondo, A., 2009. A simple and immediate method for simultaneously evaluating expression level and plasmid maintenance in yeast. J Biochem. 145, 701-708. https://doi.org/10.1093/jb/mvp028.